LEVERAGING FREELY AVAILABLE REMOTE SENSING AND ANCILLARY DATASETS FOR SEMI-AUTOMATED IDENTIFICATION OF POTENTIAL WETLAND AREAS USING A GEOGRAPHIC INFORMATION SYSTEM (GIS)

By

Benjamin R. Felton

Thesis submitted to the faculty of the University of Virginia
in partial fulfillment of the requirements for the degree of

MASTER OF SCIENCE
In
Civil Engineering

Thornton Hall B228
351 McCormick Road,
P.O. Box 400742
Charlottesville, VA, 22904
(504)982-4620
brf2er@virginia.edu

July 5, 2015

LEVERAGING FREELY AVAILABLE REMOTE SENSING AND ANCILLARY DATASETS FOR SEMI-AUTOMATED IDENTIFICATION OF POTENTIAL WETLAND AREAS USING A GEOGRAPHIC INFORMATION SYSTEM (GIS)

Benjamin R. Felton

Jonathan L. Goodall, Advisor
Department of Civil Engineering

ABSTRACT

Conducting environmental assessments for federal and state agencies is an integral part for many transportation construction projects. Wetlands are a particular environmental feature that could potentially be affected by construction projects. The identification of wetland locations can be accomplished in a variety of ways, ranging from less involved, lower accuracy methods to highly involved, higher accuracy methods. Past efforts to develop wetland identification methods are lacking in one or more of the following ways: inadequate use of ancillary data, little automation, not leveraging freely available data, excessive computation times, or requiring software not typically available within transportation agencies. This study aims to address these issues by developing a Geographic Information System (GIS)-based wetland identification tool. The aim of the tool is screening for potential wetland areas that can be further investigated by more detailed wetland identification and survey methods. Therefore, the tool is designed to minimize the number of false negatives, which are cases where the tool incorrectly designates an area as non-wetland when a wetland does in fact exist. Applying the tool to a study region with detailed wetland delineations available shows that the tool was able to identify potential wetland locations with 69.3% agreement, 24.3% false positives, and only 6.4% false negatives. Decision makers can use the prediction confidence levels generated by the tool to balance tradeoffs between the size of the area determined to be potential wetland area and the percentage of false positive prediction errors within the study area.

Table of Contents

List of Figures

List of Tables

List of Equations

Acknowledgements

I would like to thank the University of Virginia and Department of Civil and Environmental Engineering for the opportunity to conduct research on topics of interest to me. I would like to thank Dr. Jonathan L. Goodall for the guidance and support through a big portion of my academic career and Dr. Brian L. Smith for the support for our entire research group. I would also like to thank Dr. G. Michael Fitch of VCTIR for his assistance coordinating with VDOT input and Dr. Jennie L. Moody for her assistance with addressing the environmental sciences aspect of this thesis topic.

1 Introduction

1.1 Background

Wetlands are a vital natural feature inherently capable of many beneficial hydrological and environmental processes. Some of these benefits include storm water runoff control, effluent and sediment control, and providing habitats for wildlife and plants. Many wetlands have been destroyed or repurposed for agricultural or development purposes (Ouyang, Becker, Shaver, & Chen, 2013). Because of this practice, approximately half of America's original wetlands no longer exist (Klemas, 2011). The need to protect wetlands is now well known and required through federal law and regulation.

There are a wide number of different wetland types, such as marshes, swamps, bogs, and fens, with variations in soils, topography, climate, hydrology, water chemistry, and vegetation based on geographic locations (Cowardin, Carter, Golet, & Laroe, 2013). Despite the large number of wetland types, they all share basic characteristics that are used to describe wetland areas (ACoE, 1987). While field-based identification will always be necessary to conclusively identify wetlands, there is the potential to use datasets available through federal and state agencies and within a Geographic Information Systems (GIS) to determine potential wetland areas. The National Wetland Inventory (NWI) provides one example of doing such an analysis, however it is widely acknowledged that NWI, being a national-scale data product, often lacks the accuracy required to support transportation decision-making.

A number of wetland regulations have been created for the purpose of avoiding unnecessary wetland destruction. There are a number of ordinances that govern the protection and prevention of destruction for wetlands by both federal and state agencies (Table 1). As a result of these regulations, any roadway development project done by State DOT's must consider a number of alternative paths or

corridors. Each of these potential corridors are evaluated on a number of criteria, one of which is the corridor's environmental impact, in particular, the area of wetlands that would be expected to be destroyed during construction. This process is to facilitate the selection of the particular corridor that minimizes the environmental offset from construction. DOT's must sufficiently prove that the selected corridor for a project meets this criteria, showing that it is the Least Environmentally Destructive Practical Alternative (LEDPA) by providing wetlands delineations. The US Army Corps of Engineers (ACoE) evaluates these corridors as the governing authority in wetland delineation. This process is referred to as jurisdictional determination. If the LEDPA corridor is selected, the DOT will have federal approval for construction.

Program or Act	Year	Implementing agency	Description
River and Harbors Appropriation Act	1899	ACoE	Prohibits obstruction of alteration of navigable waters
Migratory Bird Hunting and Conservation Stamps	1934	FWS	Aquires wetland easements from revenue of duck stamps
Federal Aid in Wildlife Restoration Act	1937	FWS	Provides grants to States for aquiring, restoring, and maintaining wildlife areas
River and Harbors Act	1938	ACoE	Due regard must be given to wildlife conservation during water project planning
Wetlands Loan Act	1961	FWS	Provides interest free loans for wetlands acquisition and easements
Land and Water Conservation Fund Act	1964	FWS, NPS	For aquiring wildlife areas
National Environmental Policy Act	1969	All federal agencies	Requires an environmental impact statement (EIS) for federal actions affecting the environment
Ramsar Convention (Treaty)	1973	FWS	Maintains a list of wetlands of international importance
Endangered Species Act	1973	FWS	Protects threatened and endangered wildlife, fish, and plant species often found in wetlands
Executive Order 11990	1977	All federal agencies	Requires federal agencies to minimize impacts on wetlands
Clean Water Act, Section 404	1977	ACoE, EPA, FWS	Regulates the discharge of dredge or fill material into the waters
US Tax Code Tax Reform Act	1986	IRS	Provies tax edutions for wetlands donors and nonprofit organizations
Emergency Wetlands Resources Act	1986	FWS	Pay debts from the FWS for wetlands acquisition
North American Wetlands Conservation Act	1989	FWS	Provides matching grants to public/private organizations to protect, retore and enhance wetlands
Food, Agriculture, Conservation, and Trade Act	1990	NRCS	Subsidizes restoration of croplands to wetlands
Surface Transportation Revenue Act	1991	USDOT	Authorizes funding for wetland mitigation banks for state DOTs
Transportation Equity Act for the 21st Century	1998	USDOT	Funding includes restoration of previous wetland loss and wetland mitigation banking

*ACoE - Army Corps of Engineers, CWS - Canadian Wildlife Service, EPA - Environmental Protection Agency, FWS - Fish & Wildlife Services, IRS - Internal Revenue Service, NPS - National Park Service, NRCS - National Resources Conservation Service, USDOT - United States Department of Transportation

Table 1: List of federal regulations pertaining to wetlands

Current practices for identifying wetlands for LEDPA assessments can range from simple methods of referring to a publicly available datasets, such as the NWI to highly advanced and involved methods, such as the use of image analysis and geospatial software to execute a composite of different weighted classification techniques. Although referencing NWI is the simplest and easiest route, wetland locations may be incorrectly identified or missed for a variety of reasons including the fact that NWI is a national-

scale product and therefor may miss wetlands at the spatial scale required for transportation corridor assessments. Alternatively, more advanced methods for wetland identification may use much higher resolution data with a series of classification methods. This can also prove to be problematic due to time constraints. As the resolution and intensity of the classification technique increase, computation time and required resources increase as well. This will have an adverse effect to streamlining projects by slowing the delivery of tasks and increasing costs for high resolution data acquisition. Although there are a number of methods and techniques for identifying potential wetland locations remotely, none have attempted to automate this procedure for large scale projects using freely available geospatial datasets.

1.2 Purpose and Scope

The purpose of this research is to develop a wetland identification tool that makes use of freely available geospatial datasets to identify potential wetland locations at a spatial-scale relevant for transportation corridor assessments. Wetland identification can be a challenging and expensive process for state DOTs, particularly for projects covering a large geographic extent. Research has shown an opportunity to improve the wetland identification process used by DOTs by leveraging newly available remote sensing techniques and Geographic Information Systems (GIS) (Ghobadi et al., 2012; Ozesmi & Bauer, 2002). This study advances this past work by (1) using only freely available public datasets and (2) creating a tool that automates many of the data processing steps required to transform input datasets into a map of potential wetland locations. If these tools can be used by DOTs for wetland identification early in the planning phase of a project, it could offer several benefits such as reduced man-hours in the field (and associated costs of field studies), expedited approval, and streamlined project delivery.

1.3 Organization of Thesis

The remainder of this thesis is organized as follows. Section 2 contains a Literature Review, which outlines the current techniques and datasets used for wetlands identification, as well as current

practices used by a variety of state Departments of Transportation for wetland identification. Section 3 contains the Methods for using the wetland identification tool for a case study region including (1) the study area, (2) the preliminary steps for preparing datasets for the tool, (3) the required data structure hierarchy expected by the wetland identification tool, and (4) processes used within the tool. Section 4 contains Results and Discussion describing the output from the tool for the case study region and an assessment of the tools accuracy compared to on-the-ground surveyed wetlands. Section 5 contains Conclusions outlining the findings of this study and suggestions for future work.

2 Literature Review

2.1 Overview of Wetlands Identification Models

Classification methods used in remote sensing involve identifying features from their spectral signature and/or characteristics. Classification methods are broken into two subcategories: unsupervised and supervised. The classification process will designate certain pixels of a raster to a particular class based on the pixels spectral properties and/or characteristics (Lu & Weng, 2007). Unsupervised classification is used to find statistical relationships within the data to create a user specified number of land cover types. To accomplish this, clusters representing land cover types are created. Accuracy of the unsupervised classification is increased with the use of a larger number of clusters. However, this may result in splitting one land class designation into multiple clusters that would need to be merged. Although unsupervised classification is able to identify a number of land cover types, there is still some confusion in distinguishing wetland vegetation and shrubs from upland vegetation. The supervised method utilizes training data, generally ground truth data, to develop a characteristic signature for each land cover dataset for a particular region. To accomplish this, manually specified training datasets are designated for the supervised classification algorithm to reference (Lu, Mausel, Brondízio, & Moran, 2003; Lu & Weng, 2007; Tana, Letu, Cheng, & Tateishi, 2013).

Supervised classification can also utilize object oriented neighborhood analysis to define the vegetative class of a pixel relative to adjacent pixels' classification (Yan, Mas, Maathuis, Xiangmin, & Van Dijk, 2006). The following focal analysis can be used to execute neighborhood analysis: Most Significant Component (MSC), Weighted Sum of Components (WSC), and Combined Dominants (CD). MSC will return the most frequent pixel classification within a given search radius in order to filter out noise. WSC will sum values designated to pixels based on their likelihood to occur in wetlands within a determined radius. Pixels with a high likelihood of occurring in wetlands coincide with higher values, meaning that

the summation of the pixels within the determined radius gives an indication of the likelihood that the area contains wetland vegetation. CD considers a pixel as a wetland if 50% or more of the neighboring pixels are considered acceptable for wetland classification as well. These wetlands are mapped by their characteristic spectral signatures indicating color, reflectance, and texture, which can be ascertained through training datasets. Based on a review of the literature, nearest neighborhood supervised classification, primarily Maximum Likelihood, appears to be the most commonly used classification method for wetland identification.

Classification and processing software is available to assist with the classification procedure. Below is an outline of programs and classifications used in related literature. However, this is not an exhaustive list and some software are capable of a number of different classification methods. ERDAS, developed by Hexagon Geospatial, is capable of performing both unsupervised and supervised techniques using a number of variations of the Maximum Likelihood and Fuzzy Logic algorithms (Mwita et al., 2013). Mwita et al. (2013) classified multispectral images using ERDAS unsupervised Iterative Self-Organizing Data Analysis (ISODATA) method. Other studies use Environmental Studies Research Institute's (ESRI) Image Classification in ArcGIS. The Image classifier provides classification methods for Maximum Likelihood, Iso Cluster Unsupervised, Class Probability, and Principle Components classification. Trimble's Definiens Developer (eCognition) is capable of nearest neighbor object oriented classification using DELPHI 2, which classifies using a combination of nearest neighborhood and fuzzy functions (Nobrega, O'Hara, & Stich, 2011). Exelis Visual Information Solutions (ENVI) can be used for the multispectral imagery geo correction and atmospheric corrections and is capable of a number of classification methods (Sugumaran, 2004). PANCHROMA can be used for pan-sharpening and gap-filling imagery (S. Lee, 2011).

2.2 Overview of Key Datasets

Classification of remote sensing imagery can be combined with other geospatial datasets into an algorithm to identify wetlands. The following geospatial datasets were identified through the literature review as common datasets used in wetland identification procedures: (i) Digital Elevation Models (DEM) and Light Detection and Ranging (LiDAR) to characterize wetlands topographical aspects, particularly the slope, curvature, canopy height and depression locations; (ii) multi and hyper spectral satellite and aerial imagery data to provide supporting detail about plant vegetation type and soil moisture using the specified bands available; (iii) National Resources Conservation Service's (NRCS) Soil Survey Geographic (SSURGO) data to characterize soils, particularly hydric soils; (iv) US Geographical Survey's (USGS) National Hydrography Dataset (NHD) to identify bodies of water; (v) the United States Fish and Wildlife Service's (USFWS) National Wetlands Inventory (NWI) (O'Hara, 2002; Stein et al., 2012). Congruent through each dataset, higher resolutions increase the ability to identify small or narrow wetland areas. The use of each of these datasets for wetland identification is further explained in the following subsections.

2.2.1 Digital Elevation Model (DEM) and DEM-derived Datasets

Digital Elevation Models (DEM) are datasets that describe topography in a raster format that is well suited for use in GIS and terrain processing tools. The USGS maintains a comprehensive elevation data product called the National Elevation Dataset (NED), which is comprised of existing LiDAR data, cartographic contour maps, photogrammetrically derived DEM's, Shuttle Radar Topography Mission (SRTM) datasets, Interferometric Synthetic Aperture Radar (IFSAR), and bathymetry (USGS, 2015). As such, the NED has a much higher likelihood of containing site specific elevation datasets. The NED has the advantage of being consistent across the US. However, due to the number of different sources used to compile this comprehensive digital elevation data, the resolution ranges from 3 meters to 90 meters depending on the specific location. Since obtaining high-resolution LiDAR data is an expensive process,

finding and accessing this data, as well as insuring complete coverage of the site, can prove to be problematic and costly (O'Hara, 2002). NOAA's LiDAR Data Archive and USGS's EarthExplorer maintain statewide LiDAR data, where availability is primarily found in coastal counties.

By utilizing these DEM datasets, hydrologic flow accumulation and direction can be ascertained using geoprocessing methods available in GIS software that look at an individual pixel values within the raster and determine flow direction by finding the neighboring pixel with the steepest slope. In the instance that no neighboring pixel is of lower elevation, this is representative of a depression where water will begin to pool until the depression is typically filled so that flow will proceed downhill as usual. These depressions are characteristic of wetland areas, causing soils and vegetation to be maintained in saturated conditions for extended periods of time. These depressions can then be extracted as a layer for use in the identification process (O'Hara, 2002). The Compound Topographical Index (CTI) can be used to ascertain the likely wetness of an area using the topography and upstream contributing area as inputs (Knight, Tolcser, Corcoran, & Rampi, 2013). Higher wetness areas correlate to a higher likelihood of being classified as a wetland. A DEM can also be used to derive the curvature, which details the concavity of an area and can be used to supplement wetlands identification (Knight et al., 2013).

2.2.2 Multi-Spectral Imagery

Multi-spectral imagery is obtained from satellites containing a number of radiometers set to read particular wavelengths, called bands, generally within the visible and infrared spectrum. Band ranges can vary depending on the particular sensors used. As can be seen from the Appendix, there are is a wide variety of satellite imagery with differently specified band ranges. This difference in band ranges can make cross platform imagery comparisons difficult. These bands can exists in the Red-Green-Blue (RGB) region, the near infrared (NIR), middle infrared (MIR), and far infrared (FIR) (O'Hara, 2002). The typical wavelengths for each of these regions are depicted in Table 1. There are a number of

satellites that provide multispectral imagery. The commonly used satellites for wetland identification are NASA's Landsat, European Space Agency's (ESA) Advanced Synthetic Aperture Radar (ASAR), Satellite Pour l'Observation de la Terre (SPOT), NOAA's Advanced Very High Resolution Radiometer (AVHRR), GeoEye's IKONOS, Indian Remote Sensing Satellite (IRS), and NASA's Moderate Resolution Imaging Spectroradiometer (MODIS) (Friedl et al., 2010; Olmanson, Bauer, & Brezonik, 2002; Sugumaran, 2004). However, these satellites capture images at varying degrees of resolution potentially too coarse for project specific locations.

Multispectral images generally go through geo rectification, geometric correction, and atmospheric correction before being used in classification algorithms. These steps are used to set a particular projection, correcting to compensate for Earth's rotation and the positioning of the satellite at the time of image capture, and correcting the spectral values from atmospheric effects that cause reflectance scattering and absorption by constituents in the atmosphere respectively (Ghobadi et al., 2012). Pan-sharpening and gap-filling are also used to prepare imagery for use in wetland identification. Pan-sharpening is the process of combining higher resolution gray-scale imagery with the lower resolution color bands to create a high resolution color image. Gap-filling is used to fill missing values within satellite imagery by using a previous year's imagery or other gapped imagery. Certain wetlands are easier to identify and the following outlines the easiest to hardest wetlands to identify using multispectral imagery: water, marshes, deciduous forested wetlands, evergreen forested wetlands, and scrub-shrub wetlands (Ozesmi & Bauer, 2002).

Utilizing a combination of bands 3, 4, and 5 (referring specifically to Landsat 7 bands); bands 2, 4, and 7; and bands 1, 2, and 3 results in improved wetlands depiction. ETM+ band 3 depicts strong chlorophyll absorption and strong reflectance for soils, ETM+ band 4 depicts the reflectance for green vegetation, and ETM+ band 5 depicts the difference between vegetation and soils. IKONOS imagery has

been found to identify aquatic vegetation better than Landsat imagery (Olmanson et al., 2002). Landsat captures bands 1 through 7 with resolutions as high as 15m, SPOT captures bands 1 through 3 and 5 with resolutions as high as 10m, AVHRR captures 1 through 5 with resolutions as high as 1km, and IRS captures 1 through 4 with resolutions as high as 23.5m, however, it is important to note that each of these satellites capture different wavelengths for each band (Ozesmi & Bauer, 2002). Higher spatial resolutions become particularly important when delineating smaller wetlands approximately less than 500 hectares, especially when dealing with long, narrow wetland regions (Mwita et al., 2013). Because of this, coarse resolution satellite imagery, including widely used Landsat imagery, has been determined to be inadequate for mapping small wetlands due to its resolution. For smaller watersheds, alternatives like the use of aerial vehicles outfitted with multispectral cameras flown at low altitudes could be explored to obtain very high resolution multispectral imagery (Ozesmi & Bauer, 2002).

Multi and Hyperspectral imagery can be used to derive the Normalized Difference Vegetation Index (NDVI). NDVI is primarily used for monitoring of vegetation density. NDVI is computed using the red wavelength from the visible spectrum and a near-infrared wavelength using the following equation.

$$NDVI = \frac{\rho_{NIR} - \rho_{red}}{\rho_{NIR} + \rho_{red}}$$

Equation 1: Normalized Difference Vegetation Index (NDVI) equation

NDVI identifies areas based on a -1 to 1 scale, where -1 represents water bodies, around 0 represents barren earth, lower positive values represent shrubs, and higher positive values represent forested areas (Ghobadi et al., 2012). Pigmentation within plant leaves is attributed to chlorophyll, where healthy vegetation contains higher amounts of chlorophyll. This results in much lower reflectance in the visible spectrum bringing the NDVI value closer to 1. Change detection is accomplished by comparing the spectral signatures of individually classified NDVI rasters for two different, but seasonally similar, dates

(Klemas, 2011). By using two dates that differ seasonally, emergent and floating vegetation, found in the spring, can be isolated from flooded emergent vegetation and open water (Ozesmi & Bauer, 2002; Shi, 2013). Wetland vegetation generally gives off a stronger NDVI signature due to water inundation, helping distinguish wetland vegetation from other potentially water stressed vegetation. Similarly, a Tasseled Cap transformation can condense 6 different bands of multispectral imagery into 3 condensed bands representing an area's greenness, wetness, and brightness. The tasseled cap method has shown more promise than using only NDVI as this method combines 6 separate bands whereas NDVI utilizes only two (Tana et al., 2013).

Region	Wavelength	Use
Violet	380–450 nm	Deep water imaging
Blue	450–495 nm	Deep water imaging
Green	495–570 nm	Vegetation and deep water imaging
Yellow	570–590 nm	Vegetation and deep water imaging
Orange	590–620 nm	Soil, vegetation, man-made objects, and water
Red	620–750 nm	Soil, vegetation, man-made objects, and water
NIR	0.75-1.4 µm	Vegetation
SWIR	1.4-3 µm	Vegetation, soil moisture, and geologic features
MWIR	3-8 µm	Vegetation, soil moisture, and geologic features
LWIR	8-15 µm	Night studies, thermal changes in water currents
FIR (Thermal)	15-1000 µm	Night studies, thermal changes in water currents
Microwave	1-1000 mm	Land and sea surface temerature, soil moisture

Table 2: Wavelength ranges for specific spectrum regions

2.2.3 Soil Survey Geographic Database (SSURGO)

SSURGO data is used to identify hydric soils, characteristic of wetland areas (O'Hara, 2002). The SSURGO dataset is comprised of a number of polygons with identifier keys that correlate to a series of relational tables. The particular table of interest is the map unit aggregate attribute (MUAGGATT), which contains the field hydric rating (HYDCLPRS) detailing a soils hydric classification, describing completely hydric, partially hydric, not hydric, or unknown soils. Drainage class - dominant condition (DRCLASSDCD),

flooding frequency - dominant condition (FLODFREQDCD), and ponding frequency - presence (PONDFREQPRS) are also used in classification (Shuchman & Court, 2009).

2.2.4 National Hydrography Dataset (NHD)

NHD contains vector datasets establishing areas for bodies of water and flow lines. Characteristically, some wetlands exist at or near flow lines; therefore incorporating NHD into a wetland identification process can improve its accuracy. Wetlands generally exist in riparian zones, which are transitional regions between a water body and land and can be determined using geoprocessing to create a buffer around these bodies of water (O'Hara, 2002). Similarly, the Federal Emergency Management Agency (FEMA) provides Standard Digital Flood Insurance Rate Maps (DFIRMs) that contain a number of recurrence intervals that give a much better approximation of riparian zones than a simple buffer tool.

2.2.5 National Wetlands Inventory (NWI)

The current NWI derives wetland polygons using aerial imagery and detailed on-the-ground inspection data using trained image analysts to identify and locate wetland and deep-water habitats. Updates to NWI can be made from user submission of FGDC compliant wetlands data layers from external sources, which will inevitably be included in the NWI upon being approved by the US Fish and Wildlife Service (USFWS). The USFWS disseminates this information using an online mapper, an Open GIS Consortium compliant Web Map Service (WMS), and is viewable in Google Earth using Keyhole Markup Language (KML). The NWI coverage extends to the contiguous U.S., Hawaii, Puerto Rico, the Virgin Islands, Guam, the major Northern Mariana Islands, and 35% of Alaska (O'Hara, 2002).

2.3 Study of current practices

Activities by state Departments of Transportation (DOTs) concerned with the identification of wetlands as it relates to this thesis were reviewed in order to determine the state-of-the-practice in

wetland identification procedures. The list is ordered from most to least relevant in terms of the specific objectives of this thesis.

2.3.1 Colorado Department of Transportation (CDOT)

The Colorado Department of Transportation (CDOT) funded research in the development of a semi-automated method to identify and classify wetlands in the northern Front Range area of Colorado. The method uses four imagery products; NAIP, Landsat 7 ETM+, Terra ASTER, and EO-1 Hperion/ALI. Landsat data was primarily used to derive various vegetative indices and the soil crust index. EO-1 was used to create spectral signatures for the various vegetative types. The method begins by completing a rapid assessment using the ISODATA unsupervised classification. This classification breaks data into spectral clusters based on the statistical correlation of the raster data, which is followed by manual treatment of the clusters, and finally labels are assigned. The study found that the ISODATA unsupervised classification was adequate in determining possible wetland locations; however, there seems to be some confusion between wetlands and irrigated agricultural regions.

The ISODATA classification is then used in an object-based classification method. This method utilized Definiens Developer to execute the object-based classification with the nearest neighborhood classification using all ASTER bands, all Landsat bands, all EO1 bands, derive tasseled cap transformation rasters, NDVI derived from ASTER, NDVI derived from EO1, a stream buffer raster of 165m indicative of floodplain areas, a stream buffer raster of 32m indicative of marsh areas, and the wetlands layer generated from the ISODATA method. This technique classifies numerous land classes beyond wetlands including; aquatic bed, commercial/industrial zone, farm land, floodplain forest, forest, golf course, grassland, marshes, residential area, rocks, scrub/shrub, water body, and wet meadow. The overall accuracy of the method reaches 83% with accuracies in the following and class categories; marshes with

87.88%, wet meadows with 68.8%, aquatic bed with 62.5%, scrub/shrub with 70.6%, floodplain forest with 86.4%, and water with 100% (Hsu & Johnson, 2008).

2.3.2 North Carolina Department of Transportation (NCDOT)

North Carolina Department of Transportation (NCDOT) contributed to a study by the National Consortium for Remote Sensing in Transportation – Environmental Assessment (NCRST-E) by providing field wetland assessments adhering to the U.S. Army Corps of Engineers' wetland delineation manual. This study was conducted in collaboration with the U.S. DOT Research Special Projects Administration (RSPA) and Mississippi State University using Itres and EarthData International hyperspectral vegetation maps. The study ascertained that high-spatial, multi-temporal hyperspectral imagery, high-resolution digital elevation data, LiDAR- based digital elevation data, and SSURGO data used with neighborhood pixel analysis resulted in a cost and time saving identification and delineation method. The model for NCDOT wetland identification currently utilizes digital elevation models to derive slope, curvature, and depression rasters as well as soils and land use land cover using ArcGIS with Spatial Analyst, TauDEM, and Statistical Analysis System (SAS). Further development for this program includes increasing the accuracy within their developed models, expanding to add the ability to identify the wetland type using remote sensing, and developing models specific to tidal and marsh wetlands on a regional scale (NCDOT, 2015).

The driving factor for NCDOT to progress in using remotely sensed data to identify wetlands was the desire to reduce project delivery times and minimize costs (Weatherford, 2014). The NCDOT developed identification method is also sufficiently accurate to compare different alternatives for environmental planning. Three pilot projects were used to test the implementation of their models. Currently, the wetland identification model uses 2 points per square meter (approximately 1m resolution), unconditioned statewide LiDAR maps available from the North Carolina Floodplain Mapping

Program to create several terrain derivative maps. The model also uses SSURGO data and the most recent (2011) National Land Cover Dataset (NLCD). The accuracy assessment of the model is done by comparing three data layers: the model output, NWI datasets, and field delineations. However, no concrete numbers have been released because accuracy assessments do not currently incorporate instances of false positives.

NCDOT has indicated that terrain derivative maps do not prove to be very useful for identification in flat, agricultural regions. NCDOT is not interested in obtaining their own multi or hyperspectral data, and does not consider the inclusion of this data into their short-term goals for the development of their wetland identification model. The end goals for NCDOT are to develop an automated delineation tool for ArcGIS to identify wetland locations, reducing the need to use ground-truth field delineation to meet Least Environmentally Damaging Practicable Alternative (LEDPA) criteria through close coordination and discussion with the Army Corps of Engineers (ACoE). A group at UNC Charlotte is working with NCDOT to develop an ArcGIS tool to automate the wetland delineation process. NCDOT and the North Carolina Division of Water Quality shared the 2011 Environmental Excellence Award from the FHWA for this work.

2.3.3 Mississippi Department of Transportation (MDOT)

MDOT evaluated the feasibility of using remote sensing and geospatial technologies to streamline the NEPA process. Three coastal counties in Mississippi underwent considerable land cover and land use change. Due to large growth in urbanized areas, MDOT proposed to relocate a CSX railway and Interstate 10. NCRST-E contributed to this study by compiling historical satellite imagery, historical land cover and land use data, digital elevation data, USGS quadrangle maps, USGS digital orthophoto quarter quads (DOQQs), new high-resolution aerial imagery, new high-resolution multispectral satellite imagery, new high-resolution aerial hyperspectral imagery, and new high-resolution digital elevation

data (O'Hara & Barnwell, 2002). Satellite imagery included Quickbird and IKONOS. For the multi and hyperspectral imagery classification, two methods were considered, one a combination of unsupervised and supervised techniques and another using object-based. The combination methods utilized ERDAS Imagine to conduct an ISODATA clustering unsupervised classification, which was used to generate a set of signatures for particular classes to be used for Maximum Likelihood supervised classification. Definiens' eCognitio was use for object-based classification, using the nearest neighbor and membership functions. It was determined the unsupervised and supervised methods performed similarly, where the object-based improved the quality of the results (King & O'Hara, 2002; Repaka, Truax, Kolstad, & O'Hara, 2004).

2.3.4 Michigan Department of Transportation (MDOT)

MDOT funded a Transportation Applications of Restricted Use Technology (TARUT) project to identify areas where the environmental review process can be improved by reducing timelines. The study found the process of selecting wetland mitigation sites could be improved by incorporating a geospatially-based wetlands mitigation site suitability tool (WMSST). The tool utilizes SSURGO drainage class, flood frequency, hydric soils, and ponding frequency data as well as USGS percent slope data. The Michigan Natural Features Inventory (MNFI) also provides presetlement land cover data. The tool also uses Landsat imagery to derive topographic wetness index and soil moisture index data. Each of these data layers is considered in a weighted mean model that outputs potential wetlands mitigation locations using ArcGIS Desktop. The tool allows users to specify weightings to the data layers, where it will output a map of potential wetlands mitigation sites to the screen, allowing the user to save if desired. The study indicated that the tool successfully identified 19 of 20 known test sites acceptable for wetlands mitigation. Due to the tools time efficiency, approximately 73% of costs were cut per wetland mitigation site. (Shuchman & Court, 2009).

2.3.5 Washington State Department of Transportation (WSDOT)

Washington State Department of Transportation (WSDOT) was also involved in an NCRST-E project involving the I-405 corridor with the USDOT and NASA. The primary concern for this project was to develop land use land cover (LULC) maps for this particular corridor to assist the environmental division in their EIS procedure (Department of Transportation & National Aeronautics and Space Administration, 2002). WSDOT funded research to develop a guidebook for the use of multispectral imagery to develop LULC datasets. The study focuses on using Landsat 7 ETM+ imagery, claiming that Landsat is the ideal satellite choice because it is cheaper, has a wider coverage, and is collected more frequently. Classification clusters were broken into two levels; level 1 containing 9 clusters, level 2 containing 37 clusters. Supervised classification was utilized using parametric and non-parametric parameters. Parametric classification allowed for entire classification using mean vectors and covariance matrices and non-parametric classification resulted in gaps or confusion using maximum and minimum spectral values. Post processing is then done using manual improvement by overlaying orthophotos to extract farmland, golf courses, and rivers and streams, and by merging existing GIS data, including a USGS LULC map, census population data, road network, wetlands maps, park boundaries, and transportation networks. Four products are produced that result in varying strengths in classification. Layer 3 utilizes pan sharpened Landsat 7 ETM+ imagery and wetlands layers for us in prioritizing wetlands layers. Their accuracy assessment indicates that the classification accuracy is great for urbanized areas and water, but low for wetlands, forested areas, and farmlands. Randomly sampled comparison points yielded that wetlands had 0% accuracy, where wetlands pixel were wrongfully classified as urban or forested areas (R. Lee, Saulsbury, Lanzer, & Perez, 2004; Xiong, Lee, Saulsbury, & Lanzer, 2004).

2.3.6 Utah Department of Transportation (UDOT)

UDOT contributed to a study involving assessing the applicability of using unmanned aerial vehicles (UAVs) for highway related problems. The study focused on obtaining aerial imagery for pre and post construction scenarios to be used to classify wetlands plant species. This study used ERDAS Imagine to execute a Maximum Likelihood supervised classification on a five band reflectance image consisting of red, green, blue, NIR, and derived NDVI bands. A Fuzzy Convolution filter was used to remove salt and pepper classicization. This method achieved an overall accuracy of 62.57%. The study had the most difficulty in identifying narrowleaf and broadleaf cattails with an accuracy of 23.3% (Barfuss, Jensen, & Clemens, 2012).

2.3.7 Connecticut Department of Transportation (ConnDOT)

ConnDOT funded research investigating the use of color infrared, aerial photography, land use land cover maps, topographic and soils data to identify corridor impacts for environmental assessment for Route 275. Each of these components are scaled based on an importance factor, where they are combined and applied to a path analysis model that will determine the corridor with the minimal environmental impact. Impacts considered included surface hydrology, wildlife habitats, minimization of runoff/pollutants, preserves or archeology, highway grade, agricultural land, visual landscape, forest, urban land, and soil suitability (Kennard, Lefor, & Civco, 1980). ConnDOT also recently contacted the USFWS to update NWI maps for Connecticut using recently developed procedures. Existing soils data, updated and enhanced NWI+ databases, four-band color infrared imagery, and historical 1890's topographic maps (for historical reference) were used to conduct trained image analysis to update the NWI for Connecticut (Tiner, McGucking, & Herman, 2013).

2.3.8 Other Departments of Transportation

Iowa DOT began investigation on the use of remote sensing for environmental assessment techniques after development of a bypass around Eddyville was halted due to the project's impacts on protected species and their habitats. Iowa DOT coordinated with NCRST-E to identify known wetland locations to do in the field reconnaissance to delineate known wetlands locations and wetland flora and create spectral signatures for approximately 81 plant species. Iowa DOT also obtain 48 band hyperspectral imagery at 60cm and 1m resolution. The imagery and plant spectral signatures were then used by NCRST-E using similar methodologies as with NCDOT and NCRST-E join project to identify potential wetland locations (*NCRST–E Remote Sensing Mission to Eddyville, Iowa In Conjunction With the Iowa Department of Transportation*, 2001).

Illinois DOT responded to the questionnaire e-mail sent out to state DOT's inquiring about their wetlands identification methods using remote sensing. IDOT contracts the Illinois Natural History Survey for projects requiring wetlands delineation and INHS will utilize aerial photography, NWI, soils survey, and sometimes ground level imagery to determine where likely wetland locations will be. They then will pass this information to field surveying crews that will delineate wetlands in the field using GPS units that are ultimately turned into shapefiles and Microstation files to help determination of avoidance, minimization, and impacts.

Ohio DOT also responded to a questionnaire e-mail sent out to state DOT's inquiring about their wetlands identification methods using remote sensing. ODOT stated that they do not use any particular methodologies for identifying wetlands besides utilization of aerial imagery and current existing databases (NWI).

The Montana DOT also responded to the questionnaire e-mail sent out to state DOT's inquiring about their wetlands identification methods using remote sensing. MDT utilizes NAIP imagery, NWI, and

LiDAR for visual interpretation of wetland locations. MDT mentioned that since LiDAR has a high production cost, it is reserved for smaller projects to map topography and bathometric contours of large rivers. They mentioned problems with using NWI for wetland identification because land management practices result in the addition or removal of wetlands in their state.

Florida DOT utilized satellite imagery, particularly SPOT, to do trained image analysis along a 30-mile project corridor encompassing 91,000 acres in an undeveloped area throughout Duval County. The images obtained were 20m resolution near infrared and a computer tape with all digital information. The project focused on separating wetland vegetation from upland vegetation within the study area. This project took approximately 45 days saving 3.5 months compared to using traditional methods (Hawkins, 1990).

3 Methods

A handful of DOT's have explored the use geospatial software to automate the process of identifying potential wetlands locations. North Carolina DOT focuses on the use of high resolution LiDAR, SSURGO, and NLCD using ArcGIS to automate the process to accomplish this. Although NCDOT is focused on automating this process, the primary governing data set used is LiDAR and lacks multi or hyper spectral imagery which has been shown to increase accuracy (Laymon, Cruise, Estes, & Howell, 2001). Mississippi DOT uses satellite imagery, aerial photographs, LULC, and DEM data within ERDAS Imagine and Definiens' eCognitio to accomplish this. However, MDOT's methods make it difficult to automate the process by utilizing multiple software and require users to tend to the workflow from step to step. This method also uses multispectral imagery that is not freely available (Repaka et al., 2004). Colorado DOT utilizes the most extensive use of multi and hyper spectral imagery by using NAIP, Landsat 7 ETM+, Terra ASTER, and EO-1 Hyperion/ALI datasets. Although utilizing three different spectral imageries may slightly increase accuracy, this would result in massive computational time jumps. This method also lacks

ancillary data sets that have shown to increase accuracy in wetlands identification (Stein et al., 2012). Michigan DOT has developed a tool using SSURGO data sets and data sets derived from multispectral imagery. Although this tool is close to the level of autonomy and accuracy desired, the need for isolated derived data sets as input cause this method to hinder the usability of the tool (Shuchman & Court, 2009).

3.1 Study Area

The study area for this project is an approximate 17-mile corridor surrounding US Route 460 between the town of Zuni and the city of Suffolk (Figure 1). The analysis was done for the 26 12-digit HUCs that intersect this corridor for a total area of approximately 597,780 acres. The corridor falls within the Coastal Plains, one of five physiographic regions in Virginia. This physiographic region primarily consists of tidal marshes and tidal forests. The region also contains vernal pools, which only accumulate water during spring, making them difficult to identify during drier seasons or years. Vernal pools generally reside within forests or meadows. Pocosins are also common to this region, which generally sit on hillside plateaus accumulating acidic peat. Occasionally, pocosins may burn, resulting in a diversity of shrubby evergreens. The corridor also falls within the Middle Atlantic Coastal Plain, one of seven ecoregions in Virginia. The EPA describes this ecoregion as a flat plain with many swampy or marshy areas. Forest cover consists primarily of loblolly-shortleaf pine mixed with patches of oak, gum and cypress near major streams. The central and southwestern portions of this region are poorly drained soils whereas the northeastern portions are not as poorly drained. The central and southwestern regions account for approximately 15 percent cropland coverage, whereas the northeastern can range from 20-40 percent cropland coverage.

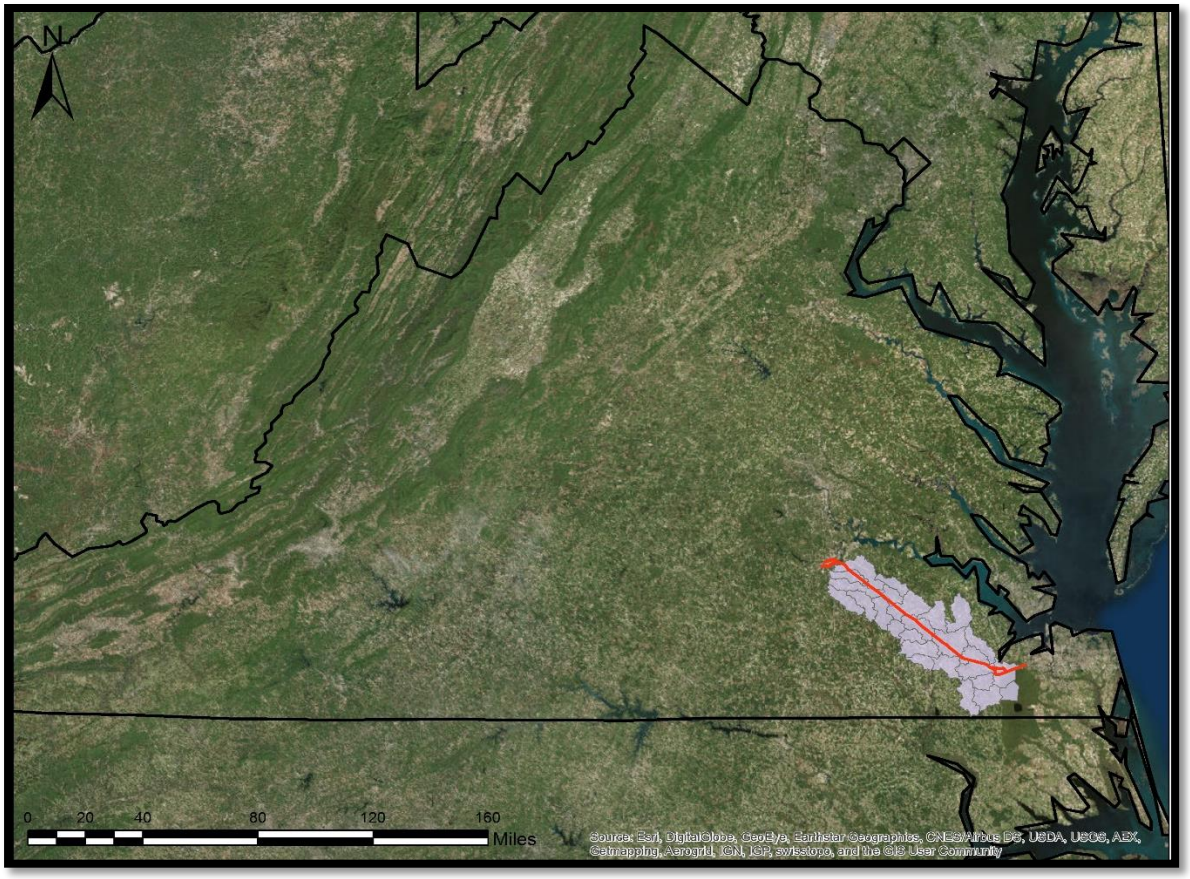

Figure 1: Site location for study showing US 460 segment and 12-Digit HUCs

3.2 Data Preparation

All datasets outlined in the following subsections were projected to the Virginia South State Plan Coordinate System in US feet. All datasets were also clipped to the previously mentioned HUCs spanning the area of interest for this study. Each process involving conversion of vectorized data to raster data and resampling of raster data utilizes the Digital Elevation Model input to set the environments for Cell Size, Snap Raster, and Extent.

3.2.1 Digital Elevation Model (DEM)

Digital Elevation Models (DEMs) provide topographical information that can be used to derive regions where there is a high likelihood for pooled water. DEMs were downloaded from the USGS's

National Map Viewer. A DEM was created using 1/9th and 1/3rd arc-second NED, which correlates to approximately 3.14 and 10.22 meter resolution respectively by downloading and merging tiles for the area of interest. The 1/3rd resolution DEM data was resampled to match the 1/9th resolution before merging together. Although DEM data was readily available for this study's area of interest, a 7,720 acre section found through 3 HUCs was left void due to the lack of 1/9th and 1/3rd resolution elevation data. This can be seen in Figure 3 towards the center of the study's area of interest. This section could have been supplemented with 1 arc-sec data, but was left blank and excluded from analysis since this study was focused on the use of higher resolution elevation datasets.

3.2.2 Federal Emergency Management Agency (FEMA) Floodplain Maps

Floodplain maps are used to identify areas of water inundation for heavy storm or flood events. 100 year floodplain maps were downloaded from FEMA's Flood Map Service Center. The 1 percent annual chance flood zone designations of Zone A, Zone AO, Zone AH, Zones A1-A30, Zone AE, Zone A99, Zone AR, Zone AR/AE, Zone AR/AO, Zone AR/A1-A30, Zone AR/A, Zone V, Zone VE, and Zones V1-V30 are all referred to as 100 year floodplain, or base flood, zones. All other zones categorized 500 year or more flood events.

3.2.3 Landsat 8 OLI Multispectral Satellite Imagery

Multispectral imagery is used to classify wetland spectral signatures and derive vegetative indices and vegetation analysis transformations from training data provided by image analysts. Landsat 8 Operational Land Imager imagery and derived products were downloaded from USGS's Earth Resources Observation and Science (EROS) Center Science Processing Architecture (ESPA) On Demand interface. This service provides a multitude of derived datasets that include conversion from digital numbers to top of the atmosphere (TOA) and surface reflectance values using the Second Simulation of a Satellite Signal in the Solar System (6S) radiative transfer models as well as atmospheric corrections

using MODIS correction routines. The Landsat 8 satellite follows the World Reference System (WRS-2) near-polar, sun-synchronous orbit. One orbit is approximately 99-minutes and provides a temporal resolution of complete coverage of the Earth every 16 days. The following table outlines the OLI bands, wavelengths, and resolutions. LandsatLook Viewer was used to identify the appropriate scenes required for this study, which is imagery from July 6, 2014 and August 14, 2014. The goal in scene selection is to identify a dates within or near the wet season. However, since precipitation rates are evenly distributed throughout the year, July was isolated as the time frame of interest due to it being historically the wettest month for the area of this study. The Scene IDs are designated as LC80140352014187LGN00 located on Path 14 and Row 35 with 10.23% cloud cover and LC80150342014226LGN00 located on Path 15 and Row 35 with 0.88% cloud cover. Ideally, we would like cloud cover to be 0%, however, from manual image interpretation, no cloud cover was present in the portion of the imagery covering the scope of this study.

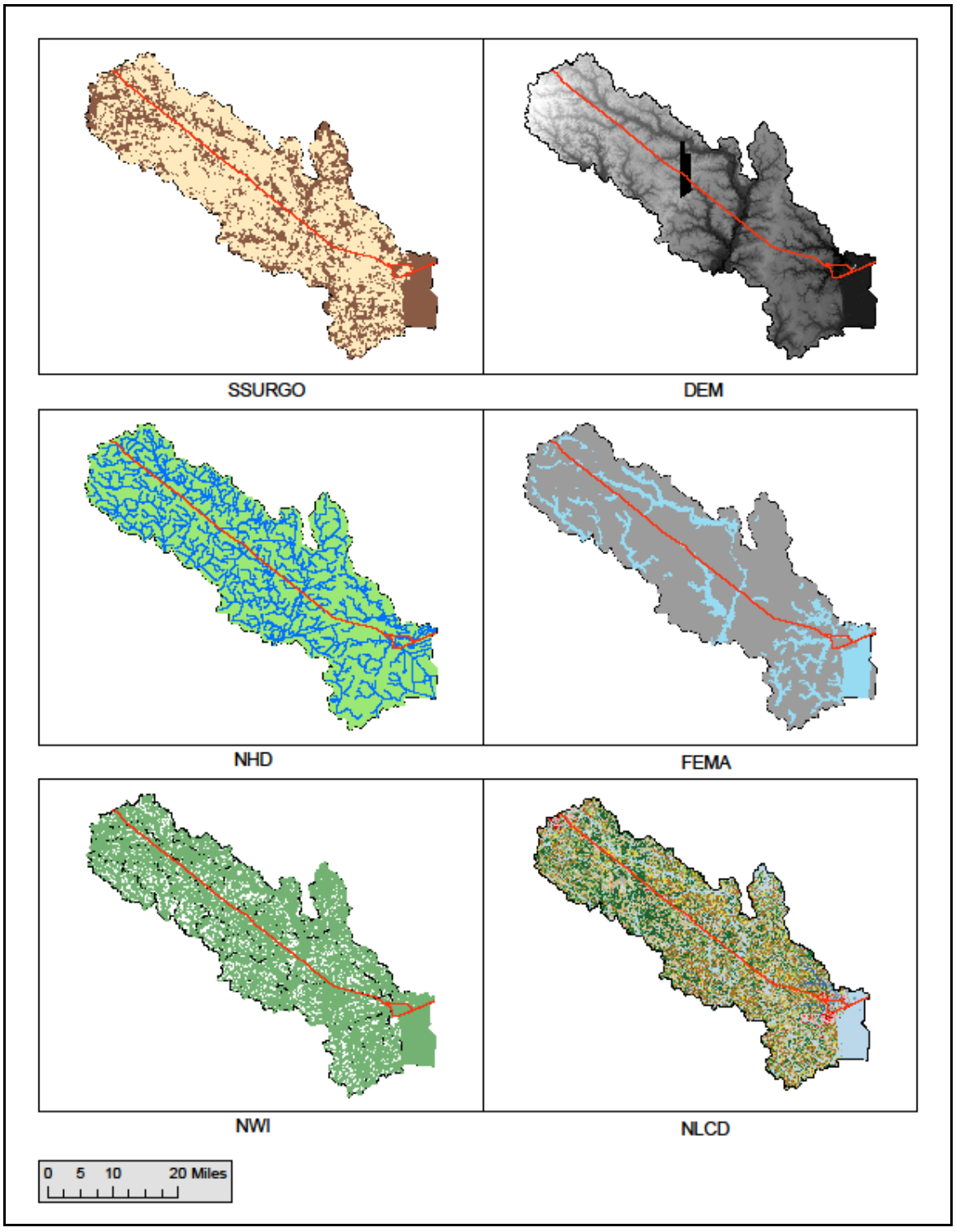

Figure 2: Grayscale images for Landsat 8 OLI bands 2 through 7

Band	Wavelength (µm)	Resolution (m)	Description
1	0.43 - 0.45	30	Coastal Aerosol
2	0.45 - 0.51	30	Blue
3	0.53 - 0.59	30	Green
4	0.64 - 0.67	30	Red
5	0.85 - 0.88	30	NIR
6	1.57 - 1.65	30	SWIR 1
7	2.11 - 2.29	30	SWIR 2
8	0.50 - 0.68	15	Panchromatic
9	1.36 - 1.38	30	Cirrus
10	10.60 - 11.19	100 (30)	TIRS 1
11	11.50 - 12.51	100 (30)	TIRS 2
*TIRS bands are acquired at 100m resolution, but are resampled to 30 meter in delivered data product			

Table 3: Landsat 8 OLI band details

3.2.4 Soil Survey Geographic database (SSURGO)

The Soil Survey Geographic database provides valuable information about soil moisture content. Wetlands regions generally consist of hydric soils. These hydric soils are provided by the SSURGO database in the form of polygon shapefiles. SSURGO datasets were downloaded from the Natural Resources Conservation Service's Web Soil Survey. Data were downloaded on a per county basis for the following counties: Isle of Wight County (VA093), Prince George County (VA149), Southampton County (VA175), Surry County (VA181), Sussex County (VA183), Chesapeake City (VA550), Dinwiddie County (VA653), and City of Suffolk (VA800). The associated Access data base (.mdb) was opened and linked to the associated *tabular* folder, which builds and loads data within the database. After building and filling the database was completed, ArcMap was used to import the *soilsmu_a_va###* polygon shapefile. The Join command was used to connect this polygon with data from the *component* table. Symbology was altered to represent the *hydricating* parameter within the *component* table. This parameter distinguishes hydric soils from non-hydric soils, which can be declared as *Yes*, *No*, or *Unknown*. This

symbolized data layer was exported to retain the hydric classification from the join. Each of the county layers were then merged into a single polygon shapefile.

3.2.5 National Hydrography Dataset (NHD)

The National Map Viewer was also used to obtain the statewide National Hydrography Dataset, which provides stream location data found in the *NHDFlowlines* subset.

3.2.6 National Land Cover Database (NLCD)

The National Land Cover Database was downloaded from the Multi-Resolution Land Characteristics Consortium's (MRLC) website.

3.2.7 National Wetlands Inventory (NWI)

The National Wetlands Inventory was downloaded from the US Fish and Wildlife Service's (USFWS) website for the entire state of Virginia.

3.2.8 Watershed Boundary Dataset (WBD)

The Watershed Boundary Dataset was downloaded for the entire United States through the USGS website where the 12-Digit HUCs covering this study's area of interest were exported into a new shapefile.

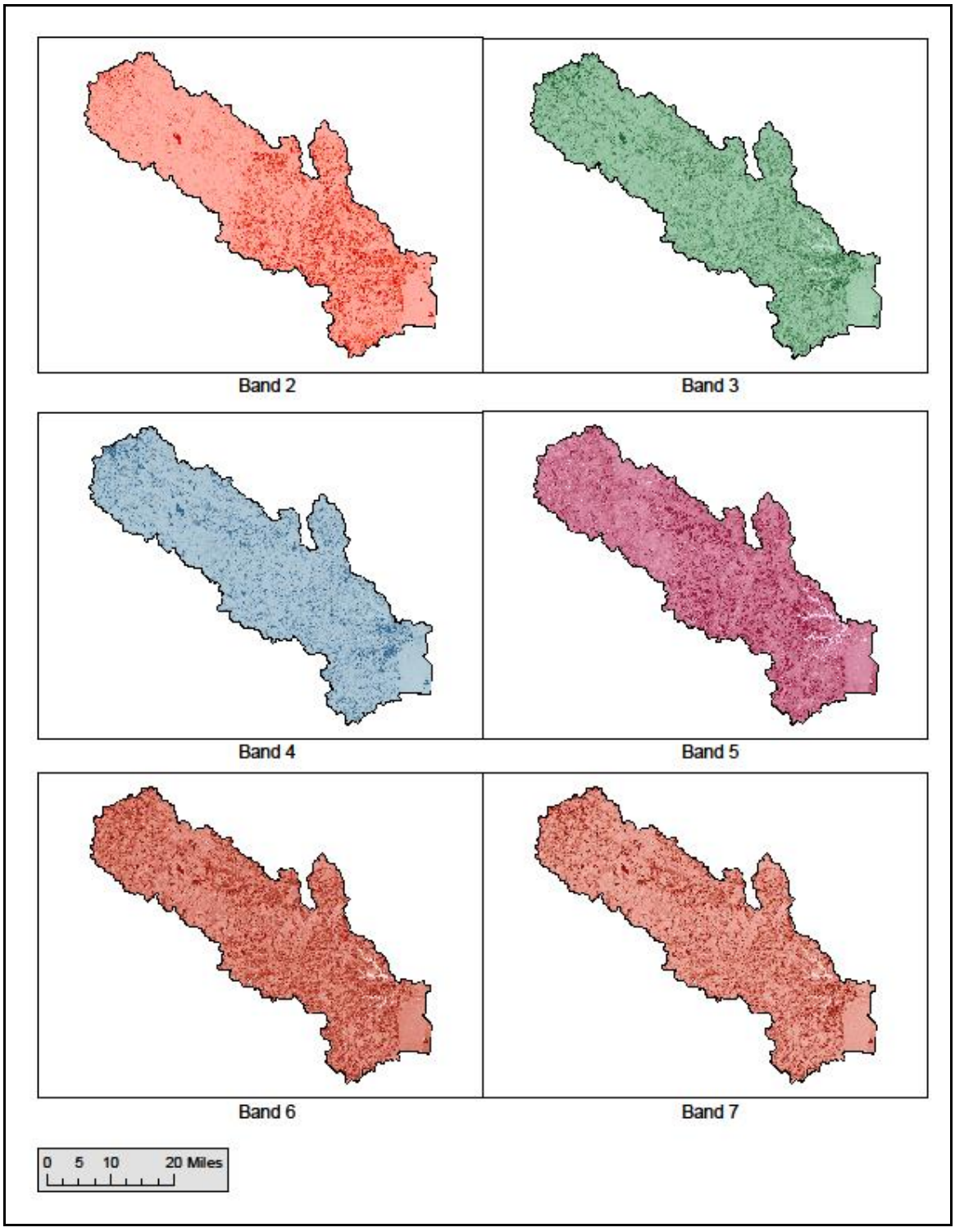

Figure 3: Images of the prepared datasets used as inputs

3.2.9 Training Data

Training data was manually created with the use of aerial imagery and NWI to quickly delineate sample locations throughout the scope of the project to encompass a variety of wetland types and characteristics to provide the classification algorithm with information about wetland signatures for each of the ancillary datasets. The image below shows a sample location of the training data depicting inland wetlands as green, river wetlands as purple, and non-wetlands as yellow.

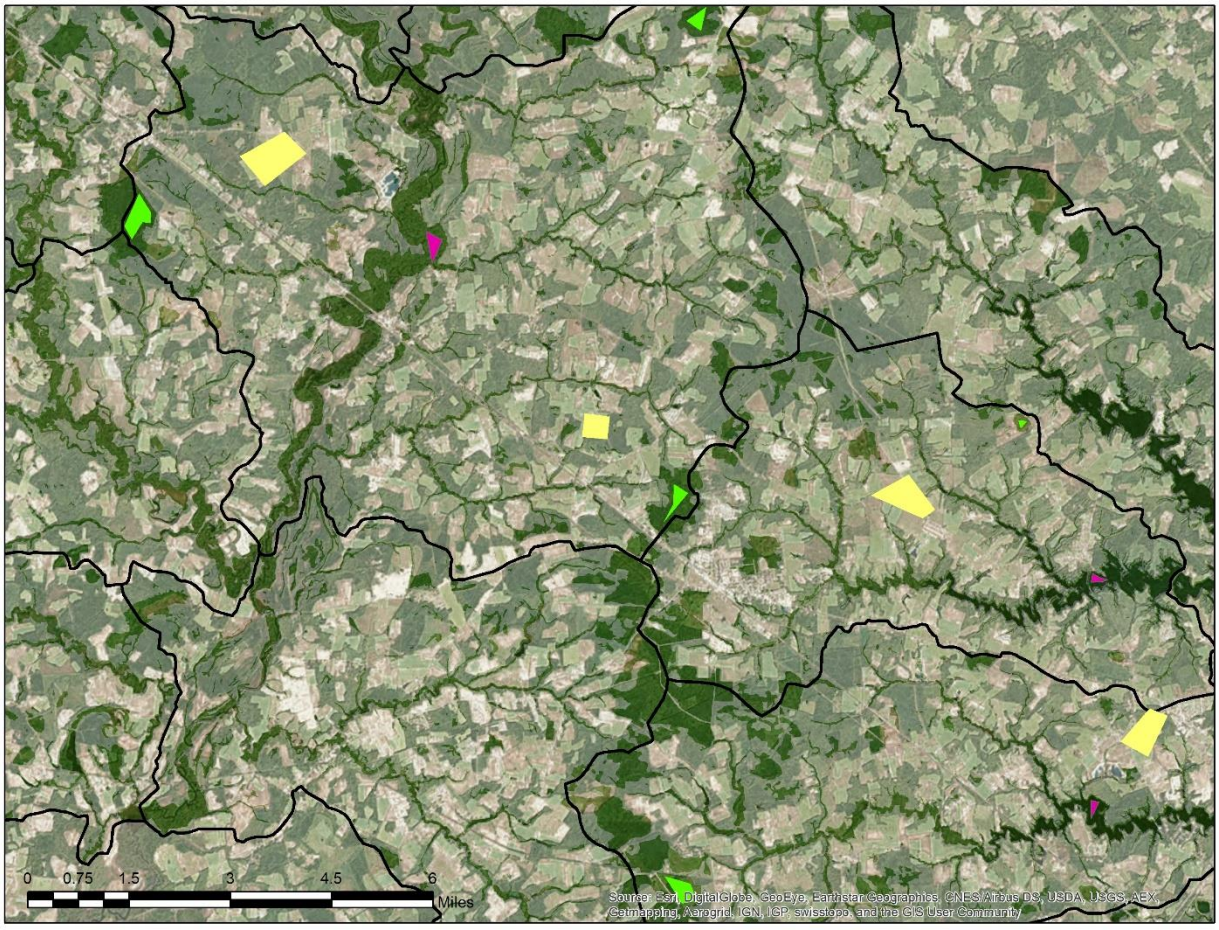

Figure 4: Training data used to train classification algorithm

3.2.10 Verification Data

Ground truth data was provided by the Virginia Department of Transportation to the study that was used to execute accuracy assessments of the tool. The data follows two potential alternative corridors for US Route 460 and was generated using trained image analysts who delineated the wetland locations manually. This data was manually delineated using a trained image analyst using color-infrared imagery, land cover maps, NWI, SSURGO, NHD, LiDAR derived DEM, and historical orthophotography, where analysts would pan the entire corridor looking at the visual cues indicating an area is wetlands.

3.3 Input Data Layout

All datasets are placed in a hierarchical structure readable by the ArcGIS tool. The following diagram outlines the structure and naming conventions for folders and files required by the tool. All datasets should be projected to the same projected coordinate system and clipped to the same boundary. This study uses the NAD 1983 Virginia South State Plane coordinate system and was clipped to the previously mentioned 12-digit HUCs. The datasets and formats required for the tool are as follows: DEM as raster data, 100-year floodplain map as polygon vector data, Landsat imagery as raster data (applicable to bands 2 through 7 from the OLI sensor), SSURGO as polygon vector data, NHD as polyline vector data, NLCD as raster data, NWI as polygon vector data, WBD HUC areas as polygon vector data, and training data as polygon vector data.

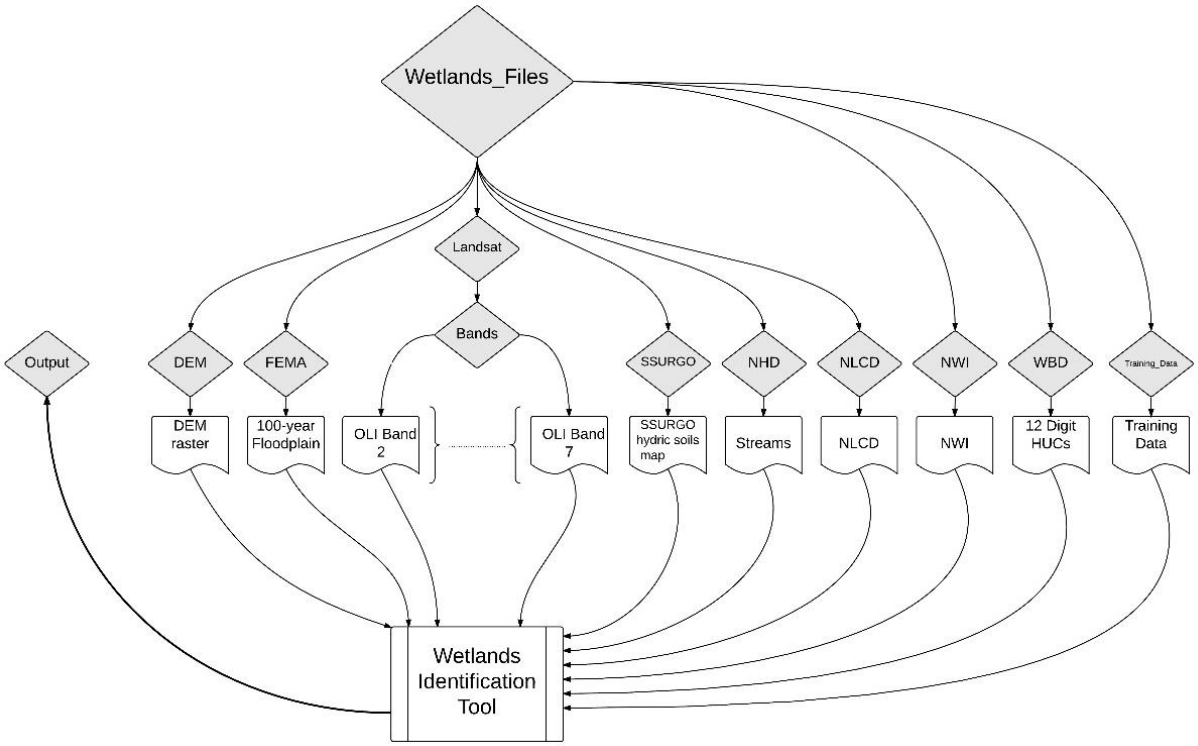

Figure 5: Image of data structure hierarchy required by the tool

3.4 Outline of tool algorithm

Because the Environmental Systems Research Institute's (ESRI) ArcGIS is a widely accepted software in the field of Geospatial Information Systems (GIS), this software was selected as the platform for the development and incorporation of the potential wetlands identification tool. This software has the capability to develop tool using ModelBuilder. ModelBuilder networks a series of tools together to allow users to run a stream of processes without requiring user input, improving the autonomy of the tool.

Although ArcGIS is capable of a number of classification methods, Maximum Likelihood was selected as it is the more accepted method for classification. The Maximum Likelihood classification requires a manually generated training dataset in order for the classification to build a spectral profile

for land cover types. Alternative classification methods include Iso Cluster, which are capable of classification without training data, however, output is organized into statistically clustered groups which then will need intensive manual post processing to merge clusters into appropriate land use land class categories. The tool uses built-in ArcMap functions to execute a work flow that results in a final land use land cover raster that identifies wetland locations.

The images below depicts the workflow of the ModelBuilder tool used for potential wetlands mapping. The tool is segmented into four sections: satellite Imagery processing, DEM raster processing, riparian zone processing, and tertiary processes that handle all other ancillary data sets.

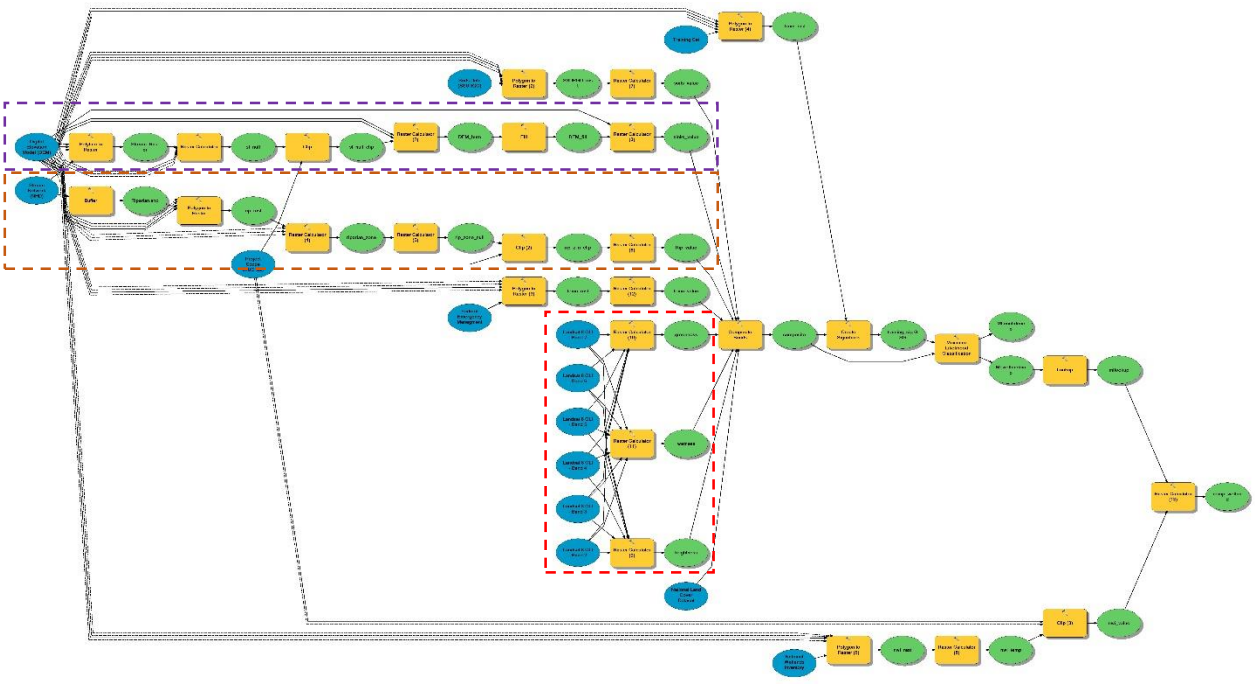

Figure 6: Flow diagram for potential wetlands identification tool. Figures 7-9 provide zoom-in views of the key components of the workflow that are highlighted with dashed lines in this figure.

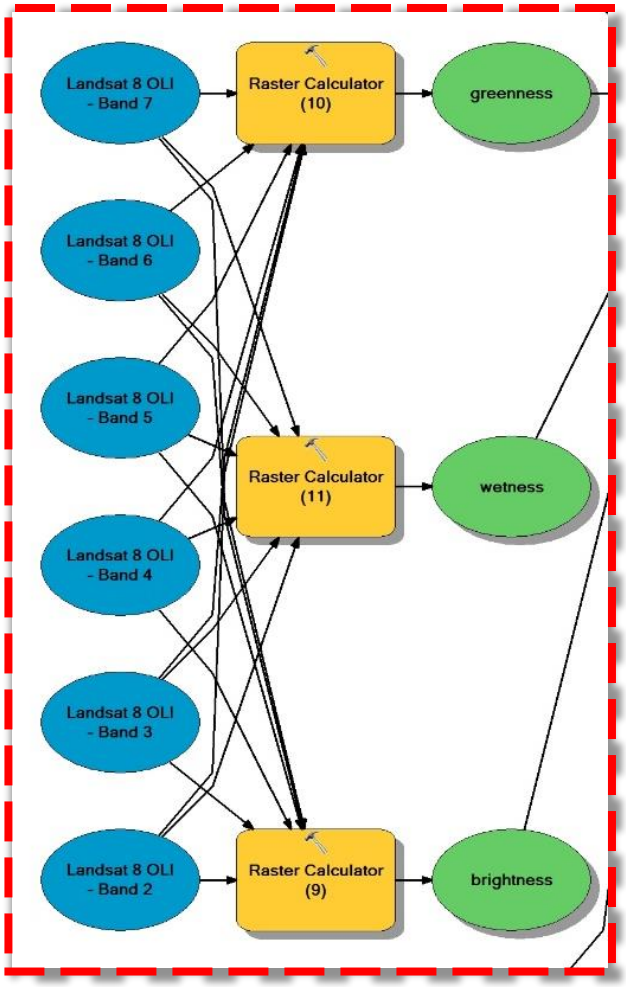

Figure 7: Satellite imagery processing

The satellite imagery processing section consist of generating three descriptive indices created from using a Tasseled Cap Transformation (TCT) on the Landsat 8 OLI imagery for bands 2 through 7. Bands 2, 3, and 4 are channels found in the visible spectrum, where bands 5, 6, and 7 are channels found in the shortwave infrared (SWIR) and near infrared spectrum (NIR). The tool utilizes these bands and condenses them into the three indices, which describe the greenness, wetness, and brightness of an areas. Each of these rasters were created using Raster Calculator and the following equations describing the weighted sum of comments method for generating these rasters. The following table outlines the scalars used for weighting each band (Hasan Ali Baig, Zhang, Shuai, & Tong, 2014).

$$Brightness = \sum_{i=2}^{7} (w_{1i} * band_i)$$

Equation 2: Brightness weighted sum of components equation

$$Greenness = \sum_{i=2}^{7} (w_{2i} * band_i)$$

Equation 3: Greenness weighted sum of components equation

$$Wetness = \sum_{i=2}^{7} (w_{3i} * band_i)$$

Equation 4: Wetness weighted sum of components equation

(Landsat 8) TCT	(Blue) Band 2	(Green) Band 3	(Red) Band 4	(NIR) Band 5	(SWIR1) Band 6	(SWIR2) Band 7
Brightness	0.3029	0.2786	0.4733	0.5599	0.5080	0.1872
Greenness	-0.2941	-0.2430	-0.5424	0.7276	0.0713	-0.1608
Wetness	0.1510	0.1973	0.3283	0.3407	-0.7117	-0.4559

Table 4: Tasseled Cap Transformation coefficients for the Landsat 8 OLI sensor

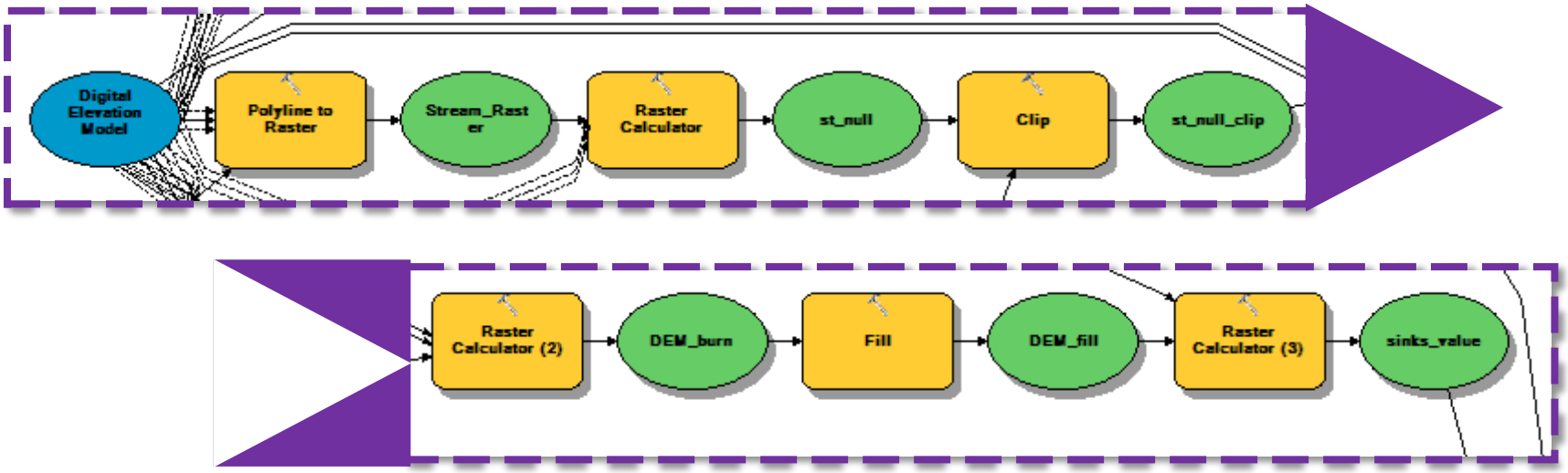

Figure 8: DEM processing

The DEM processing section uses DEM data to compute a sink raster, which identifies depressions throughout the topography. The DEM is first conditioned using NHD flow lines converted to a raster. The NHD flow line raster is multiplied by a large value, in this case 100 feet, and is subtracted from the DEM. This process is known as burning in streams. The Fill tool is then used to fill any depressions within the burned DEM. The filled and original DEM are then used in Raster Calculator, and pixels with changes in elevation are designated a value of 1 and pixels with the same elevation are designated a value of 0. The Fill tool is generally used to remove small imperfections in topography for flow path analysis, however, here it is used to identify depressed areas. Burning in streams is required to avoid cases where Fill may consider an extremely large area a depression. For example, a bridge crossing a stream would register at a higher elevation than the stream it is crossing and the Fill tool would fill all contributing areas up to the bridge, which would incorrectly lead to identifying these areas as a depressions.

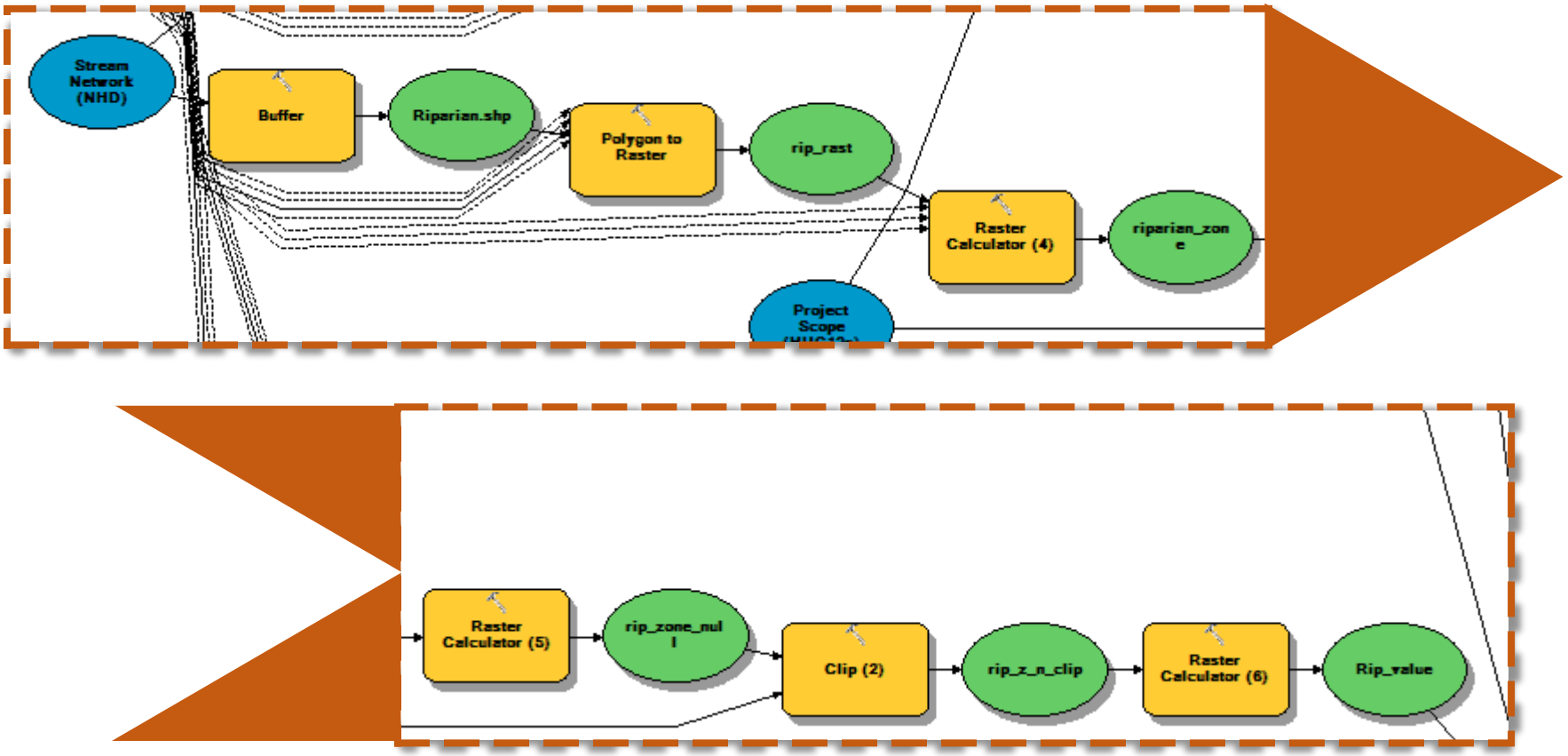

Figure 9: Riparian processing

The Riparian zone processing section creates a buffer of 100 feet surrounding each NHD flowline and converts the polygons to a raster, where raster calculator was then used to compute a binary raster where pixels within the 100 foot riparian zone are designated a value of 1 and all other areas designated a value of 0.

All tertiary processing revolves around the creation of binary rasters that represent wetlands traits. The tool assumes that the DEM is the highest resolution raster and is used as a processing constraint for the resolution, cell size, snap raster, and processing extent for all tools that involve conversion of vector data to raster data or resampling of lower resolution data. FEMA data is converted from polygon to raster. Raster Calculator is then used to compute a binary raster where pixels within the floodplain are designated a value of 1 and all other areas a value of 0. SSURGO data is converted from polygon to raster. Raster Calculator is then used to compute a binary raster where pixels containing hydric soils are designated a value of 1 and non-hydric soils a value of 0. NWI data is converted from polygon to raster. Raster Calculator is then used to compute a binary raster where pixels containing wetland areas delineated by USFWS are designated a value of 1 and non-wetland areas a value of 0. NLCD data data is incorporates as is. User generated training data is converted from polygon to raster, specifying pixels with the appropriate land use land cover designation specified.

After all previously mentioned processing is complete, the tool composites each of these rasters into a comprehensive image, with the exception of the training data and NWI data. The rasterized training areas and composite image then used to develop signatures for the particular known land classes found throughout the image. This builds a library of spectral signatures that is then used for the maximum likelihood classification, in this study's case, the land cover designations are river wetlands, inland wetlands, and non-wetlands. The result of these operations is a land use land cover raster

mapping the user specified land classes as well as a confidence raster describing the certainty of the maximum likelihood classification for 14 levels of confidence. The tool then merges the river wetlands and inland wetlands into one class and uses raster calculator to also include NWI designated wetlands.

4 Results and Discussion

4.1 Model Predictions

Figure 10 depicts two datasets that contain mapped wetlands: this study's model output and VDOT identified wetlands. The color depiction for each of the datasets are as follows: model output for wetlands is green, model output for non-wetlands is beige, and VDOT delineated wetlands are a red outline. The model performed well for region shown in Figure 10 with a low percentage of false negatives. However, there are still areas where false positives appear. The purple outline identifies a false negative where the model predicted no wetland, but the VDOT delineation identified a wetland. The blue outline identifies a false positive where the model predicted a wetland, but the VDOT delineation did not identify a wetland. In terms of this study's goals of creating a potential wetland identification map that can be used to focus survey-based identification efforts, false positives are less concerning than false negatives. It is important to note that the VDOT data only extends to the associated corridor, therefore, model verification does not extend beyond the corridor extent.

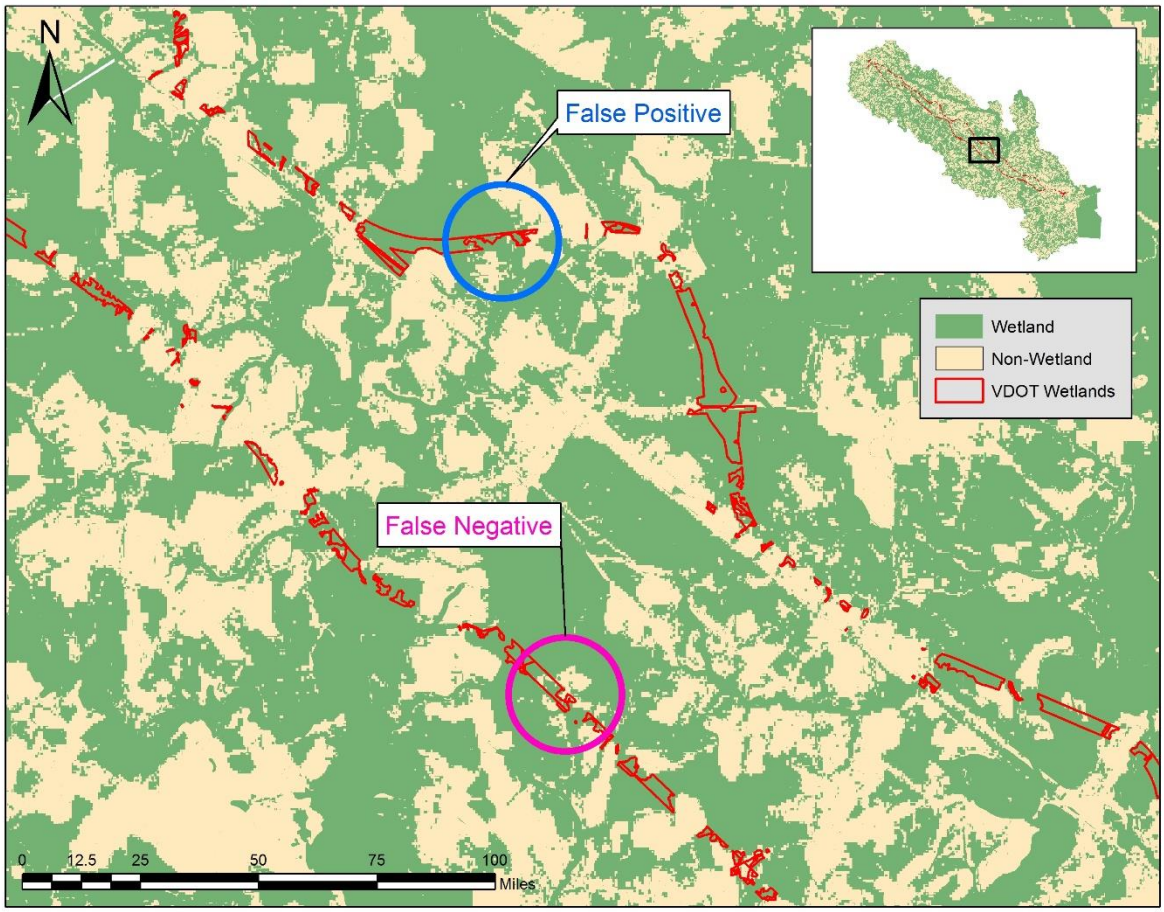

Figure 10: Survey vs model predicted wetlands

4.2 Confidence Level

Figure 11 presents the confidence raster associated with the model predictions. This raster is generate through ArcGIS's Maximum Likelihood classification and can be used to supplement the model projections for decision support applications. This raster depicts the Maximum Likelihood classification's confidence in classification of each particular pixel. The level of confidence ranges from values of 1 to 14, where lower values represent lower confidence and higher values represent higher confidence. These discrete levels where combined into 4 levels of confidence: none, low, moderate, and high. None spans values 1 to 3, Low spans values 3 to 6, Moderate spans values 6-10, and High spans values 10-14.

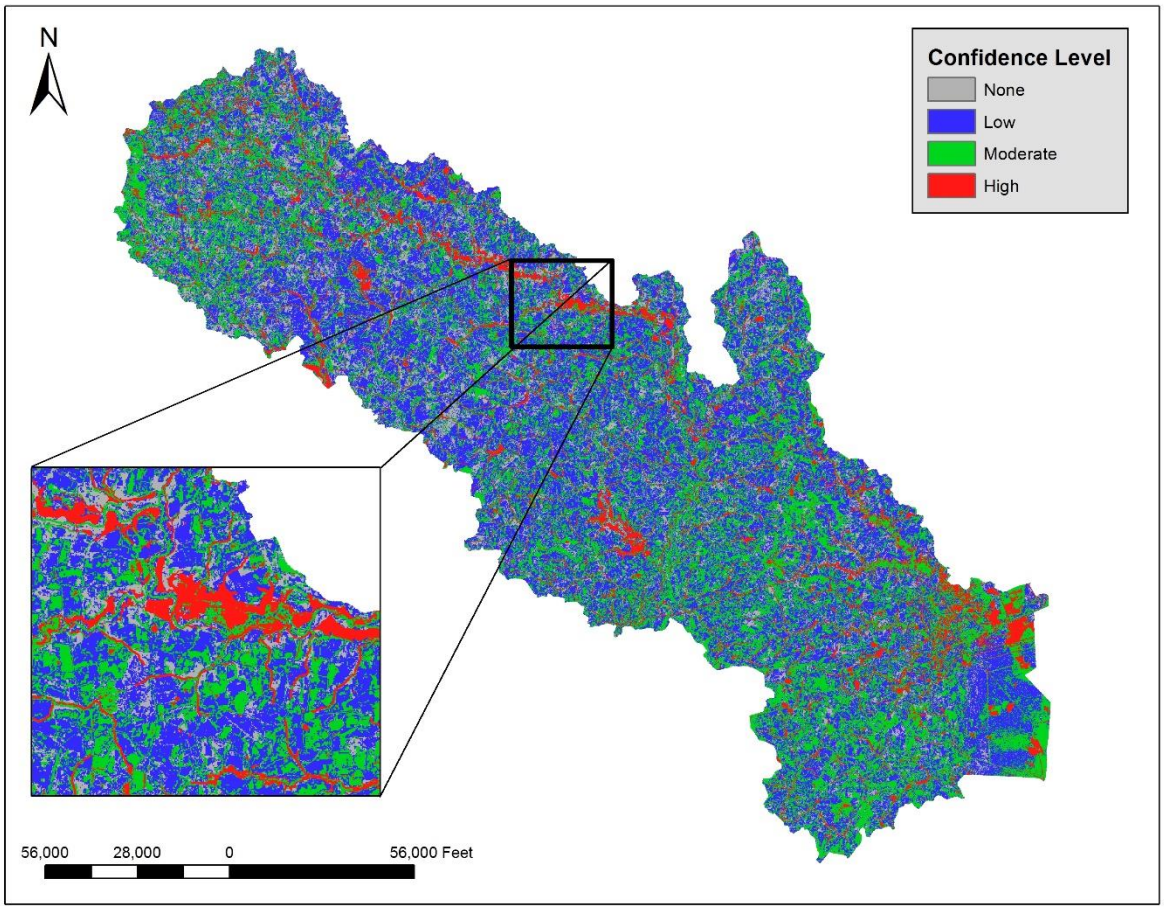

Figure 11: Grouped confidence raster

4.3 Accuracy Assessment

Figure 12 provides a comparison of the model output to VDOT mapped wetlands, which are considered the ground truth for the accuracy assessment. The figure was generated by using a raster difference calculation. For both the model output and VDOT mapped wetlands, wetland locations are designated with a value of 1 and non-wetland areas designated with a value of 0. The ArcGIS Raster Calculator tool was used to subtract the VDOT binary rasters from the model output binary raster. This results in false negatives being assigned a value of -1, shown in red, false positive being assigned a value of 1, shown in blue, and agreement between the two rasters being assigned a value of 0, shown in green.

The tool is configured to minimize false negatives (predicting no wetland when there is in fact a wetland) in order to focus survey efforts for wetland delineation on areas that have potential wetlands. For high levels of accuracy in identifying as many actual wetlands locations as possible, reducing the number of false negatives is extremely important, whereas minimizing the number of false positives is much less important. The tool can be reconfigured to meet other objectives, such as minimizing both false positives and false negatives if simple prediction of actual wetlands is the primary need of the decision maker.

In Figure 12, the bottom left images are focused on two prominent problem areas found within the model output where false negatives were high. Future work should be directed to better understanding the reason for these clustered regions of false negative predictions. Potential reasons for these errors include either in accuracies in the “ground truth data” or missing information in the wetland identification algorithm. To verify the accuracy in the “ground truth” dataset, on the ground field work should be done to double check that the areas are truly wetland areas. If the area is verified to be wetlands, then there may be unique characteristics of these locations that could be incorporated into the prediction tool to remove these false negative predictions. It is also possible that there have been recent land changes in these regions that are not reflected in the underlying datasets used in the prediction tool.

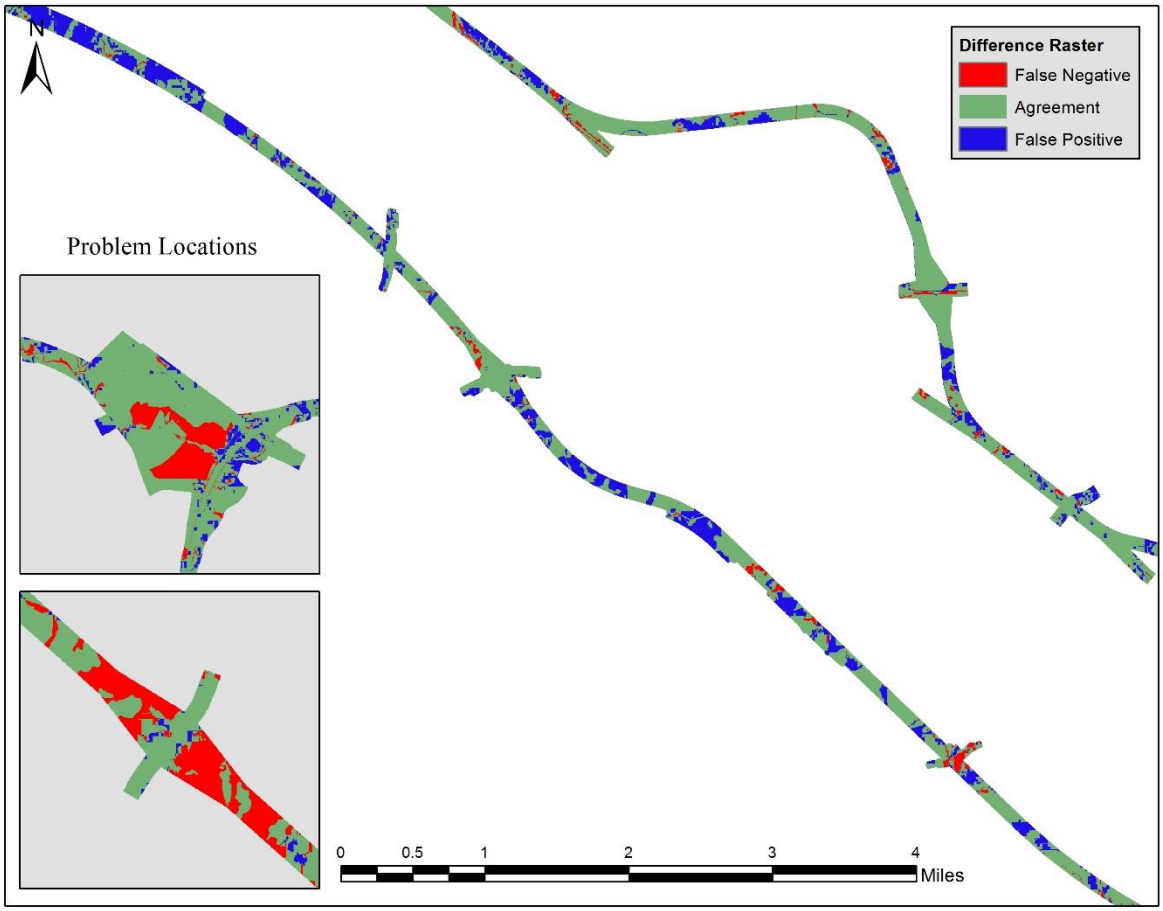

Figure 12: Difference raster

Table 5 outlines the total area for false negatives, false positives, and agreement pixels. The tool agreed with the VDOT wetland delineations for 69.3% of the study area. For the remaining portion of the study region, the majority of this area included false positive errors (24.3%) where the model predicted a wetland, but no wetland existing according to the VDOT delineation. Only 6.4% of the study region resulted in false negatives. Again, because the primary goal of the tool is to minimize false negatives, this 6.4% is the best reflection of the "accuracy" of the model. If this tool was used as a preliminary screening tool that focused wetland delineation efforts in potential wetland areas identified

by the tool, then while this would streamline delineation efforts by reducing the area required for wetland delineation, 6.4% of the wetlands in the study area would have been missed.

	Area within both corridors	
	Area (acre)	Percent Area (%)
False Negatives	523	6.4
Agreement	5669	69.3
False Positives	1984	24.3

Table 5: Difference raster areas

4.4 Utilizing Model Predictions with Confidence Level

Figure 13 presents a composite of the model predictions with the confidence level added for false negative areas. The confidence level provides important information to decision makers that can be used when determining the benefits and costs of focusing wetland delineation efforts to streamline projects. For example, if a high level of confidence is needed, then the decision maker may wish to survey all pixels that have a minimal, low, or moderate confidence level, even if the tool determined these pixels to be non-wetland areas. This would increase the total area that required surveying, therefore increasing the cost and time required to complete the surveying, but it would reduce the number of missed wetland areas. Table 6 provides the area within each confidence level for the false negative predictions along with its percentage of the total site area and the percentage of false positives in that confidence level compared to the total site area. This data shows that, if all non-wetland "minimal confidence" and "low confidence" regions were included in the wetland delineation survey, it would have resulted in the need to survey 2,584 more acres (31.6% of the study region). At the same time, it would have reduced the false negatives from 6.4% of the study region to 2.9% of the study region.

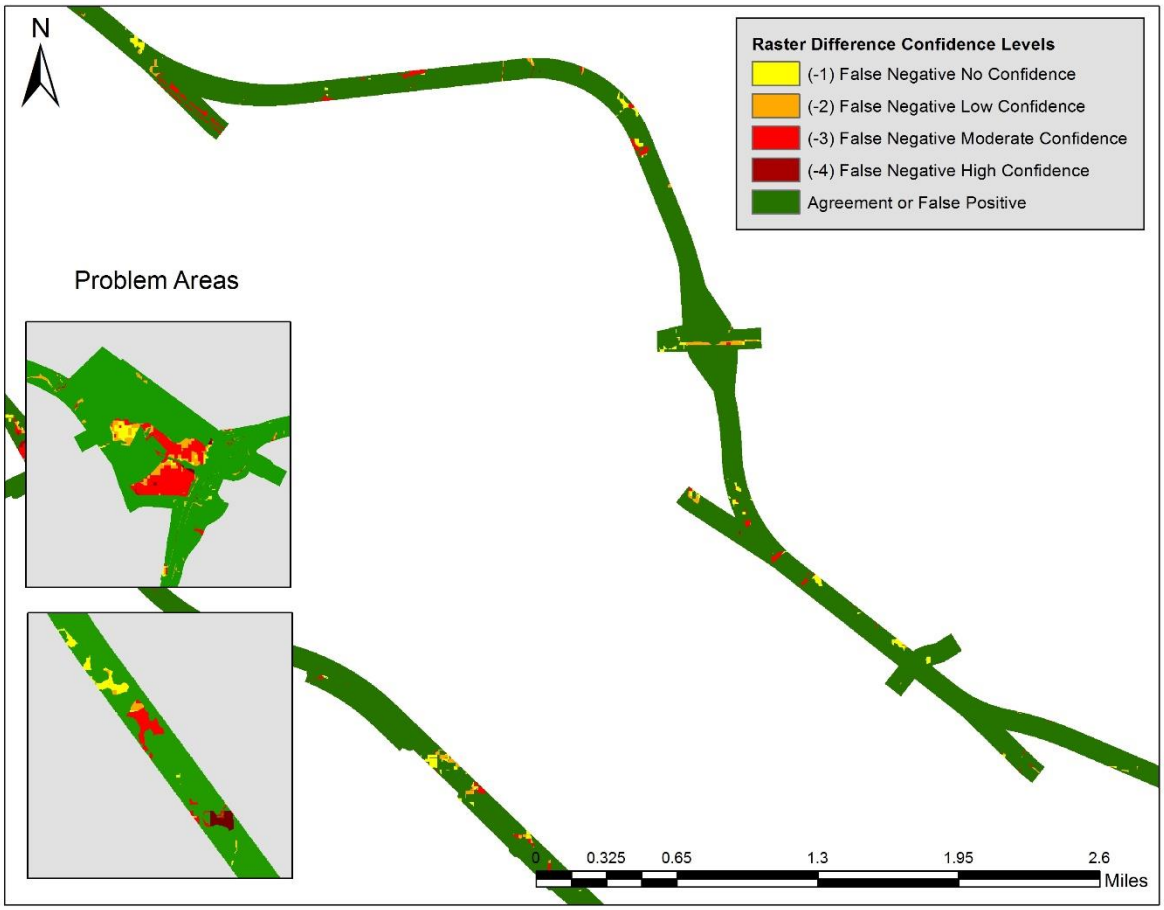

Figure 13: Difference raster supplemented with confidence levels

	Area (acre)	Percent Area (%)	Percent False Positives (%)
Minimal Confidence	781	9.5	1.90
Low Confidence	1803	22.1	1.56
Moderate Confidence	1834	22.4	2.86
High Confidence	123	1.5	0.09

Table 6: Difference/Confidence raster areas

Figure 14 further describes this trade-off between reducing the number of false negative predictions and increasing the area of the study region that must be surveyed. Given that the area of the region that must be surveyed is a surrogate for the cost and time required to complete the wetland

delineation, this figure illustrates the trade-off between error (false positives) and cost (survey area) for the study region. Given this information, a decision maker may elect to reduce the percentage of false negatives from 6.4% to 4.5% by surveying an additional 9.5% of the project site area. The additional 9.5% of the site area that would be surveyed are pixels that were classified as non-wetland, but with only minimal confidence. This relationship between error and cost may be specific to this study region and further work applying the wetland identification tool and performing surveyed wetland delineation for other regions would be necessary to gain insight into the regional variability of the error vs cost relationship. If a general relationship is found, it could be applied for sites without survey data to understand the potential trade- off between error and cost for the wetland identification tool.

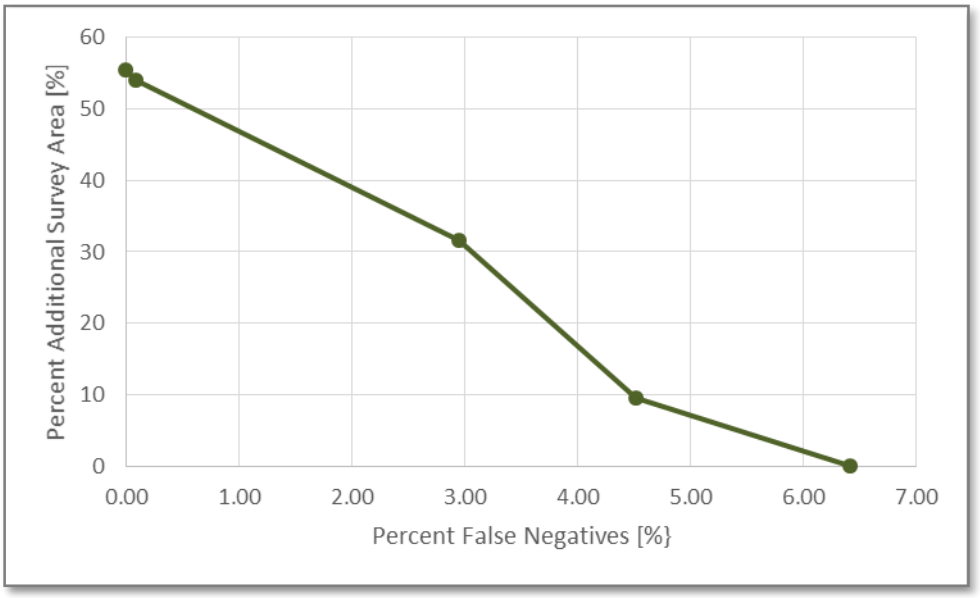

Figure 14: Relationship between level of certainty and increase surveyed areas

5 Conclusions and Future Work

5.1.1 Conclusions

The semi-autonomization of current wetlands identification techniques using freely available datasets to isolate target sites for on the ground wetlands delineation has shown great promise for

reducing man-hours in the field, expediting approval, and streamlining project delivery. By utilizing this approach, it was possible to obtain results in agreement with those from a trained image analyst's method for nearly 70% of the study region. Because the tool was configured to minimize false negatives (predicting no wetland when there is in fact a wetland), the majority of disagreement between the tool and the trained image analyst's method were cases where the tool identified a wetland when the analyst did not (false positives). Only about 6% of the study region resulted in false negatives. The tool run time took approximately 6 hours, whereas a trained image analysts may take several days, therefore it offers benefits especially if used as a screening tool to focus the efforts of the trained analyst to regions where wetlands are probable. Although the data preparation for the model would take an estimated week, the same procedures would be required when using manual identification methods. The tool has the added benefit that it could be used for other regions, given that it is based on national-scale publically available datasets.

An important part of the tool is the resulting prediction confidence raster. This information can be used to balance the trade off between error and cost for the wetland identification tool. For example, a decision maker could override the model results by electing to have a trained image analyst survey areas that have a low confidence level for its "non-wetland" prediction. Doing so would reduce the error (number of false negative predictions) but increase the cost by increasing the area that would need to be surveyed. The confidence raster also provides important insights into the predictive capability of the tool and potential areas for improvement. For example, the confidence raster indicates that the tool is easily able to identify lakes, rivers, and ocean pixels, which can be attributed to their characteristic spectral response of being highly absorptive in the near infrared bands which is a stark difference between other land cover types. Urbanized areas generally had higher classification confidence levels due to their distinctive spectral response.

The coarse spatial resolution of Landsat imagery appears to be the restrictive dataset that causes the tool to be inaccurate. The pixelated mapping of the model output edges is indicative that the multispectral imagery component of the model is governing, which is apparent in this imagery due to its coarse resolution in comparison to the other model components. Unfortunately, due to a poor spatial resolution of 30 meters, these areas can account for some error within the tools classification. The spectral response for a single pixel is associated with a 900 square meter area, which may include a number of different land cover types, resulting in a pixel value not representative of this area and result in wrongful classification.

Another source of error for the tool could be due to inaccuracies within the verification data provided. Manual inspection of the verification data cross referenced with areal imagery showed a few instances where wetland areas may have been identified incorrectly. For example, certain wetland polygon regions in the verification data intersected roadways. It is possible that these wetlands exists underneath bridge structures, which would not have been identified by the tool as wetlands locations. Alternatively, inconsistency in the time of acquisition for the model datasets and verification data can result in errors in location where drastic land cover changes occur in short periods of time. Regardless, field verification of areas where the model projections different from the survey projections would help to further refine the model.

5.1.2 Future Work

Future work should focus on increasing accuracies using higher resolution data as they become available. Digital elevation model (DEM) datasets can be replaced with higher resolution LiDAR-dervied DEM datasets in the future. With the inclusion of LiDAR data, the tool has access to drastically higher spatial resolutions, thereby increasing the detection of smaller or thinner wetlands. LiDAR also can be utilized to provide height characteristics of vegetation, which would be useful if it is necessary to type

the vegetation or wetlands. For example, differentiating between forest or scrub-shrub wetlands could be possible with this additional information.

Another advancement to this study would be to implement newer and higher resolution satellite imagery when it becomes available. GeoEye's IKONOS satellite currently can provide resolutions up to 1m, but the data can be expensive. Advancements in satellite imagery are increasing at a swift pace, so increases in spatial and spectral resolution are not far away and, as a result, may parallel increases in resolution with freely available imagery as well. Also, newer satellites are offering hyperspectral imagery, which will drastically increases the number of available bands, giving the ability to develop more continuous spectral profiles.

Satellites are also pushing advancement into longer wavelengths, particularly the microwave region. Soil Moisture Active Passive (SMAP) is one such satellite that operates in the microwave wavelengths and is capable of penetrating atmospheric and canopy disturbances to evaluate surface soil moisture levels. This data can be extremely beneficial to supplement SSURGO soil information. While soil hydrologic groups are important for wetland identification, soil moisture, which is difficult to obtain now for broad regions, would be a critical dataset for identifying wetland locations given that wetlands will have very high soil moisture profiles relative to neighboring locations.

Another potential area of improvement would be the use of Unmanned Areal Vehicles (UAV) rather than satellites for data collection. Using UAVs has the advantage of operating at lower elevations, avoiding most atmospheric disturbances, to obtain extremely high spatial resolutions. It may also be possible to obtain more up-to-date data using UAVs compared to satellites. There are challenges with this approach, however, including changing regulations and a nascent commercial market for UAV services. It is projected that the use of UAVs for a variety of purposes including environmental

monitoring will increase in the future, and if so, UAV derived data could be used in a tool like the one developed in this research to improve its accuracy at identifying potential wetland locations.

6 References

Barfuss, S. L., Jensen, A., & Clemens, S. (2012). *Evaluation and Developent of Unmanned Aircraft (UAV) for UDOT Needs*.

Department of Transportation, & National Aeronautics and Space Administration. (2002). *Achievements of the DOT-NASA Joint Program on Remote Sensing and Spatial Information Technologies: Application to Multimodal Transportation*.

Friedl, M. a., Sulla-Menashe, D., Tan, B., Schneider, A., Ramankutty, N., Sibley, A., & Huang, X. (2010). MODIS Collection 5 global land cover: Algorithm refinements and characterization of new datasets. *Remote Sensing of Environment*, *114*, 168–182. doi:10.1016/j.rse.2009.08.016

Ghobadi, Y., Pradhan, B., Kabiri, K., Pirasteh, S., Shafri, H. Z. M., & Sayyad, G. A. (2012). Use of multi-temporal remote sensing data and GIS for wetland change monitoring and degradation. In *IEEE Colloquim on Humanities, Science & Engineering Research* (pp. 103–108). doi:10.1109/CHUSER.2012.6504290

Hasan Ali Baig, M., Zhang, L., Shuai, T., & Tong, Q. (2014). Derivation of a tasselled cap transformation based on Landsat 8 at-satellite reflectance. *International Journal of Remote Sensing*, *5*(5), 423–431. doi:10.1080/01431160110106113

Hawkins, H. (1990). Eye in the Sky: Satellite Imagery Aids Florida DOT. *Public Works*, *121*(8).

Hsu, C., & Johnson, L. E. (2008). Multi-Criteria Wetlands Mapping Using an Integrated Pixel-Based and Object-Based. *Colorado Department of Transportation*, (CDOT-2008-8).

Kennard, W. C., Lefor, M. W., & Civco, D. L. (1980). Identification of Inland Wetlands for Transportation Planning Using Color Infrared Aerial Photography, *Final Repo*.

King, R. L., & O'Hara, C. G. (2002). A synthesis of remote sensing applications for environmental assessment. In *paper in the proceedings of the Pecora*. Retrieved from http://www.ncrste.msstate.edu/archive/publications/conference/pecora/final_papers/A_SYNTHESIS_OF_REMOTE_SENSING_APPLICATIONS_FOR_ENVIRONMENTAL_ASSESSMENT.pdf

Klemas, V. (2011). Remote Sensing of Wetlands: Case Studies Comparing Practical Techniques. *Journal of Coastal Research*, *27*(May), 418–427. doi:10.2112/JCOASTRES-D-10-00174.1

Knight, J. F., Tolcser, B. P., Corcoran, J. M., & Rampi, L. P. (2013). The Effects of Data Selection and Thematic Detail on the Accuracy of High Spatial Resolution Wetland Classifications. *Photogrammetric Engineering & Remote Sensing*, *79*(July), 613–623.

Laymon, C., Cruise, J., Estes, M., & Howell, B. (2001). *TECHNOLOGY GUIDE : NCRSTE _ TG001 Assessing the Need for Remote Sensing Information to Conduct Environmental Assessment in Transportation*.

Lee, R., Saulsbury, J. B., Lanzer, E. L., & Perez, A. (2004). Guidance on Using Remote Sensing Applications for Environmental Analysis in Transportation Planning. *Washngton State Department of Transportation*, (WA-RD 593-2).

Lee, S. (2011). *Detecting Wetland Change through Supervised Classification of Landsat Satellite Imagery within the Tunkwa Watershed of British Columbia , Canada Steven Lee*.

Lu, D., Mausel, P., Brondízio, E., & Moran, E. (2003). Change detection techniques. *International Journal of Remote Sensing*, *25*(12), 2365–2401. doi:10.1080/0143116031000139863

Lu, D., & Weng, Q. (2007). A survey of image classification methods and techniques for improving classification performance. *International Journal of Remote Sensing*, *28*(March), 823–870. doi:10.1080/01431160600746456

Mwita, E., Menz, G., Misana, S., Becker, M., Kisanga, D., & Boehme, B. (2013). Mapping small wetlands of Kenya and Tanzania using remote sensing techniques. *International Journal of Applied Earth Observation and Geoinformation*, *21*, 173–183. doi:10.1016/j.jag.2012.08.010

NCDOT. (2015). North Carolina Department of Transportation. Retrieved January 1, 2015, from http://www.ncdot.gov/

NCRST–E Remote Sensing Mission to Eddyville, Iowa In Conjunction With the Iowa Department of Transportation. (2001).

Nobrega, R. A. A., O'Hara, C., & Stich, B. (2011). Top-down landscape-based approach toward the assess and rank watershed and wetlands impacted by transportation corridor. In *Transportation Research Board*.

O'Hara, C. G. (2002). *Technology Guide: NCRSTE_TG003 Remote Sensing and Geospatial Application for Wetlands Mapping, Assessment, and Mitigation*.

O'Hara, C. G., & Barnwell, C. (2002). Coordinating and Managing Remote Sensing and Spatial Technology Information for Environmntal Assessment in Transportation Projects. In *27th Annual Meeting of the National Association of Environmental Professionals* (pp. 1–17).

Olmanson, L. G., Bauer, M. E., & Brezonik, P. L. (2002). Aquatic Vegetation Surveys Using High-Resolution Ikonos Imagery. In *Future Intelligent Earth Observing Satellite System Conference*.

Ozesmi, S. L., & Bauer, M. E. (2002). Satellite remote sensing of wetlands. *Wetlands Ecology and Management*, *10*, 381–402. doi:10.1023/A:1020908432489

Repaka, S. R., Truax, D. D., Kolstad, E., & O'Hara, C. G. (2004). Comparing spectral and object based approaches for classification and transportation feature extraction from high resolution multispectral imagery. In *ASPRS Annual Conference Proceedings*. doi:10.1.1.84.3803

Shi, Y. (2013). *A Remote Sensing and GIS-based Wetland Analysis In Canaan Valley , West Virginia*.

Shuchman, R., & Court, G. (2009). Developing and Applying a Geospatial Decision Support Tool for Efficient Identification of Wetlands Mitigation Sites. *Transportation Research Record*, *10-1870*.

Stein, B. R., Zheng, B., Kokkinidis, I., Kayastha, N., Seigler, T., Gokkaya, K., … Hwang, W. H. (2012). An Efficient Remote Sensing Solution to Update the NCWI. *Photogrammetric Engineering & Remote Sensing*, (June), 537–547.

Sugumaran, R. (2004). *Using Remote Sensing Data to Study Wetland Dynamics in Iowa*.

Tana, G., Letu, H., Cheng, Z., & Tateishi, R. (2013). Wetlands mapping in north america by decision rule classification using MODIS and ancillary data. *IEEE Journal of Selected Topics in Applied Earth Observations and Remote Sensing*, *6*(December), 2391–2401. doi:10.1109/JSTARS.2013.2249499

Tiner, R. W., McGucking, K., & Herman, J. (2013). *Potential Wetland Restoration Sites for Connecticut: Results of a Preliminary Statewide Survey*.

USGS. (2015). U.S. Geologic Survey: About NED. Retrieved from http://ned.usgs.gov/about.html

Weatherford, M. (2014). *NCDOT WETLAND MODELING PROGRAM UPDATES Presented at the Interagency Coordination*.

Xiong, D., Lee, R., Saulsbury, J. B., & Lanzer, E. L. (2004). *Remote Sensing Applications for Environmental Analysis in Transportation Planning : Application To the Washington State I-405 Corridor*.

Yan, G., Mas, J. -F., Maathuis, B. H. P., Xiangmin, Z., & Van Dijk, P. M. (2006). Comparison of pixel-based and object-oriented image classification approaches—a case study in a coal fire area, Wuda, Inner Mongolia, China. *International Journal of Remote Sensing*, *27*(September), 4039–4055. doi:10.1080/01431160600702632

7 Appendix

EO-1 ALI

Bands	Wavelength (µm)	Resolution (m)
Pan	0.48 - 0.69	10
MS - 1'	0.433 - 0.453	30
MS - 1	0.45 - 0.515	30
MS - 2	0.525 - 0.605	30
MS - 3	0.63 - 0.69	30
MS - 4	0.775 - 0.805	30
MS - 4'	0.845 - 0.89	30
MS - 5'	1.2 - 1.3	30
MS - 5	1.55 - 1.75	30
MS - 7	2.08 - 2.35	30

EO-1 Hyperion

Bands	Average Wavelength (nm)	Resolution (m)
B1	355.59	30
B2	365.76	30
B3	375.94	30
B4	386.11	30
B5	396.29	30
B6	406.46	30
B7	416.64	30
B8	426.82	30
B9	436.99	30
B10	447.17	30
B11	457.34	30
B12	467.52	30
B13	477.69	30
B14	487.87	30
B15	498.04	30
B16	508.22	30
B17	518.39	30
B18	528.57	30
B19	538.74	30
B20	548.92	30
B21	559.09	30
B22	569.27	30

B23	579.45	30
B24	589.62	30
B25	599.8	30
B26	609.97	30
B27	620.15	30
B28	630.32	30
B29	640.5	30
B30	650.67	30
B31	660.85	30
B32	671.02	30
B33	681.2	30
B34	691.37	30
B35	701.55	30
B36	711.72	30
B37	721.9	30
B38	732.07	30
B39	742.25	30
B40	752.43	30
B41	762.6	30
B42	772.78	30
B43	782.95	30
B44	793.13	30
B45	803.3	30
B46	813.48	30
B47	823.65	30
B48	833.83	30
B49	844	30
B71	851.92	30
B50	854.18	30
B72	862.01	30
B51	864.35	30
B73	872.1	30
B52	874.53	30
B74	882.19	30
B53	884.7	30
B75	892.28	30
B54	894.88	30
B76	902.36	30
B55	905.05	30
B77	912.45	30
B56	915.23	30

B78	922.54	30
B57	925.41	30
B79	932.64	30
B58	935.58	30
B80	942.73	30
B59	945.76	30
B81	952.82	30
B60	955.93	30
B82	962.91	30
B61	966.11	30
B83	972.99	30
B62	976.28	30
B84	983.08	30
B63	986.46	30
B85	993.17	30
B64	996.63	30
B86	1003.3	30
B65	1006.81	30
B87	1013.3	30
B66	1016.98	30
B88	1023.4	30
B67	1027.16	30
B89	1033.49	30
B68	1037.33	30
B90	1043.59	30
B69	1047.51	30
B91	1053.69	30
B70	1057.68	30
B92	1063.79	30
B93	1073.89	30
B94	1083.99	30
B95	1094.09	30
B96	1104.19	30
B97	1114.19	30
B98	1124.28	30
B99	1134.38	30
B100	1144.48	30
B101	1154.58	30
B102	1164.68	30
B103	1174.77	30
B104	1184.87	30

B105	1194.97	30
B106	1205.07	30
B107	1215.17	30
B108	1225.17	30
B109	1235.27	30
B110	1245.36	30
B111	1255.46	30
B112	1265.56	30
B113	1275.66	30
B114	1285.76	30
B115	1295.86	30
B116	1305.96	30
B117	1316.05	30
B118	1326.05	30
B119	1336.15	30
B120	1346.25	30
B121	1356.35	30
B122	1366.45	30
B123	1376.55	30
B124	1386.65	30
B125	1396.74	30
B126	1406.84	30
B127	1416.94	30
B128	1426.94	30
B129	1437.04	30
B130	1447.14	30
B131	1457.23	30
B132	1467.33	30
B133	1477.43	30
B134	1487.53	30
B135	1497.63	30
B136	1507.73	30
B137	1517.83	30
B138	1527.92	30
B139	1537.92	30
B140	1548.02	30
B141	1558.12	30
B142	1568.22	30
B143	1578.32	30
B144	1588.42	30
B145	1598.51	30

B146	1608.61	30
B147	1618.71	30
B148	1628.81	30
B149	1638.81	30
B150	1648.9	30
B151	1659	30
B152	1669.1	30
B153	1679.2	30
B154	1689.3	30
B155	1699.4	30
B156	1709.5	30
B157	1719.6	30
B158	1729.7	30
B159	1739.7	30
B160	1749.79	30
B161	1759.89	30
B162	1769.99	30
B163	1780.09	30
B164	1790.19	30
B165	1800.29	30
B166	1810.38	30
B167	1820.48	30
B168	1830.58	30
B169	1840.58	30
B170	1850.68	30
B171	1860.78	30
B172	1870.87	30
B173	1880.98	30
B174	1891.07	30
B175	1901.17	30
B176	1911.27	30
B177	1921.37	30
B178	1931.47	30
B179	1941.57	30
B180	1951.57	30
B181	1961.66	30
B182	1971.76	30
B183	1981.86	30
B184	1991.96	30
B185	2002.06	30
B186	2012.15	30

B187	2022.25	30
B188	2032.35	30
B189	2042.45	30
B190	2052.45	30
B191	2062.55	30
B192	2072.65	30
B193	2082.75	30
B194	2092.84	30
B195	2102.94	30
B196	2113.04	30
B197	2123.14	30
B198	2133.24	30
B199	2143.34	30
B200	2153.34	30
B201	2163.43	30
B202	2173.53	30
B203	2183.63	30
B204	2193.73	30
B205	2203.83	30
B206	2213.93	30
B207	2224.03	30
B208	2234.12	30
B209	2244.22	30
B210	2254.22	30
B211	2264.32	30
B212	2274.42	30
B213	2284.52	30
B214	2294.61	30
B215	2304.71	30
B216	2314.81	30
B217	2324.91	30
B218	2335.01	30
B219	2345.11	30
B220	2355.21	30
B221	2365.2	30
B222	2375.3	30
B223	2385.4	30
B224	2395.5	30
B225	2405.6	30
B226	2415.7	30
B227	2425.8	30

B228	2435.89	30
B229	2445.99	30
B230	2456.09	30
B231	2466.09	30
B232	2476.19	30
B233	2486.29	30
B234	2496.39	30
B235	2506.48	30
B236	2516.59	30
B237	2526.68	30
B238	2536.78	30
B239	2546.88	30
B240	2556.98	30
B241	2566.98	30
B242	2577.08	30

GeoEye-1 GIS-MS

Bands	Wavelength (µm)	Resolution (m)
Panchromatic	0.450-0.800	0.46
Blue	0.450-0.510	1.84
Green	0.510-0.580	1.84
Red	0.655-0.690	1.84
Near Infra Red	0.780-0.920	1.84

GeoEye-1 IKONOS-2

Bands	Wavelength (µm)	Resolution (m)
Panchromatic	0.760-0.850	0.82
Blue	0.455-0.520	3.2
Green	0.510-0.600	3.2
Red	0.630-0.700	3.2
Near Infra Red	0.760-0.850	3.2

Landsat 7 ETM+

Bands	Wavelength (µm)	Resolution (m)
Band 1	0.45-0.52	30
Band 2	0.52-0.60	30
Band 3	0.63-0.69	30
Band 4	0.77-0.90	30
Band 5	1.55-1.75	30
Band 6	10.40-12.50	60 * (30)
Band 7	2.09-2.35	30
Band 8	.52-.90	15

Landsat 8 OLI

Bands	Wavelength (µm)	Resolution (m)
Band 1 - Coastal aerosol	0.43 - 0.45	30
Band 2 - Blue	0.45 - 0.51	30
Band 3 - Green	0.53 - 0.59	30
Band 4 - Red	0.64 - 0.67	30
Band 5 - Near Infrared (NIR)	0.85 - 0.88	30
Band 6 - SWIR 1	1.57 - 1.65	30
Band 7 - SWIR 2	2.11 - 2.29	30
Band 8 - Panchromatic	0.50 - 0.68	15
Band 9 - Cirrus	1.36 - 1.38	30
Band 10 - Thermal Infrared (TIRS) 1	10.60 - 11.19	100 * (30)
Band 11 - Thermal Infrared (TIRS) 2	11.50 - 12.51	100 * (30)

Orbview-3

Bands	Wavelength (µm)	Resolution (m)
Pan	0.450-0.900	1
MS1 (Blue)	0.450-0.520	4
MS2 (Green)	0.520-0.600	4
MS3 (Red)	0.625-0.695	4
MS4 (NIR)	0.760-0.890	4

SPOT 7

Bands	Wavelength (µm)	Resolution (m)
Panchromatic	0.450-0.745	1.5
Blue	0.450-0.520	1.5
Green	0.530-0.590	1.5
Red	0.625-0.695	1.5
Near Infrared	0.760-0.900	1.5

Quickbird

Bands	Wavelength (µm)	Resolution (m)
Panchromatic	0.405-1.053	0.55
Blue	0.430-0.545	2.16
Green	0.466-0.620	2.16
Red	0.590-0.710	2.16
Near-IR	0.715-0.918	2.16

RapidEye

Bands	Wavelength (µm)	Resolution (m)
Blue	0.440-0.510	5
Green	0.520-0.590	5
Red	0.630-0.685	5
Red Edge	0.690-0.730	5
NIR	0.760-0.850	5

SkySat-2

Bands	Wavelength (µm)	Resolution (m)
Blue	0.450-0.515	2
Green	0.515-0.595	2
Red	0.605-0.695	2
Near Infra-Red	0.740-0.900	2

Terra ASTER

Bands	Wavelength (µm)	Resolution (m)
1	0.52-0.60	15
2	0.63-0.69	15
3N	0.78-0.86	15
3B	0.78-0.86	15
4	1.60-1.70	30
5	2.145-2.185	30
6	2.185-2.225	30
7	2.235-2.285	30
8	2.295-2.365	30
9	2.360-2.430	30
10	8.125-8.475	90
11	8.475-8.825	90
12	8.925-9.275	90
13	10.25-10.95	90
14	10.95-11.65	90

WorldView-3

Bands	Wavelength (µm)	Resolution (m)
Panchromatic	0.450-0.800	0.31
Coastal	0.400-0.450	1.24
Blue	0.450-0.510	1.24
Green	0.510-0.580	1.24
Yellow	0.585-0.625	1.24
Red	0.630-0.690	1.24
Red Edge	0.705-0.745	1.24
Near-IR1	0.770-0.895	1.24
Near-IR2	0.860-1.040	1.24
SWIR-1	1.195-1.225	3.7
SWIR-2	1.550-1.590	3.7
SWIR-3	1.640-1.680	3.7
SWIR-4	1.710-1.750	3.7
SWIR-5	2.145-2.185	3.7
SWIR-6	2.185-2.225	3.7
SWIR-7	2.235-2.285	3.7
SWIR-8	2.295-2.365	3.7
Desert Clouds	0.405-0.420	30
Aerosol-1	0.459-0.509	30
Green	0.525-0.585	30
Aerosol-2	0.635-0.685	30
Water-1	0.845-0.885	30
Water-2	0.897-0.927	30
Water-3	0.930-0.965	30
NDVI-SWIR	1.220-1.252	30
Cirrus	1.365-1.405	30
Snow	1.620-1.680	30
Aerosol-3	2.105-2.245	30
Aerosol-4	2.105-2.245	30